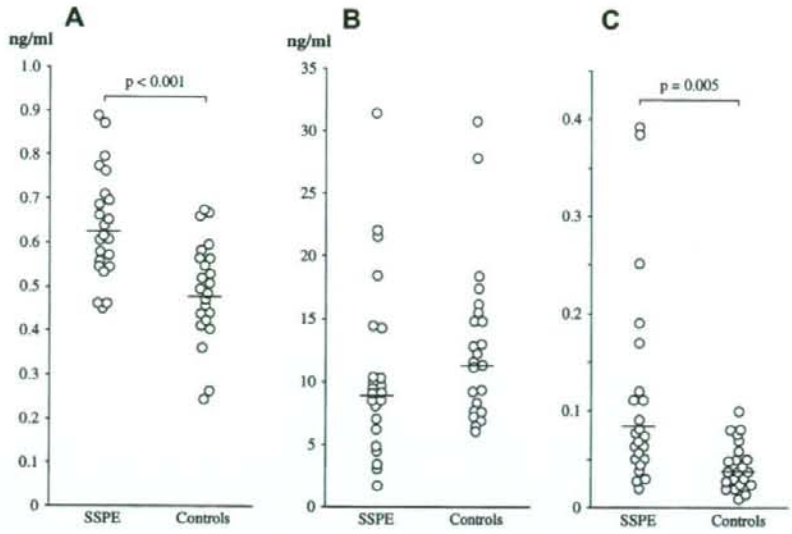

Figure 1 CSF concentrations of MMP-9 (A), TIMP-1 (B), and the ratios of MMP-9/TIMP-1 (C) in SSPE patients and controls. Horizontal lines indicate geometric means.

Statistical analysis

All data were log transformed to give an approximately normal distribution. The differences in the results between groups were analyzed using the Mann–Whitney *U* test. A *p* value <0.05 was considered significant. Correlations were analyzed using Pearson's coefficient correlation. All values are reported as geometric means. Analyses and calculations were performed using SPSS-12.0 (SPSS, Inc., Chicago, IL, USA).

Results

The geometric means of CSF MMP-9 and TIMP-1 levels, and MMP-9/TIMP-1 ratios of the controls were 0.48 ng/ml (range, 0.26–0.67 ng/ml), 11.6 ng/ml (range, 6.1–11.6 ng/ml), and 0.04 (range, 0.01–0.10), respectively (Fig. 1). The geometric means of CSF MMP-9 and TIMP-1 levels, and MMP-9/TIMP-1 ratios of SSPE patients were 0.62 ng/ml (range, 0.45–0.88 ng/ml), 8.1 ng/ml (range, 1.7–31.5 ng/ml), and 0.08 (range, 0.02–0.39), respectively (Fig. 1). CSF MMP-9

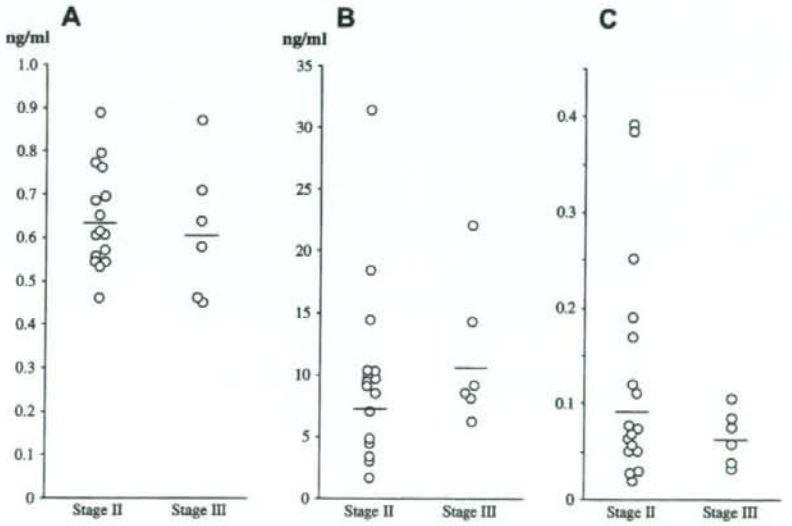

Figure 2 CSF concentrations of MMP-9 (A), TIMP-1 (B), and the ratios of MMP-9/TIMP-1 (C) in SSPE patients in Jabbour stage II and III. Horizontal lines indicate geometric means.

levels and MMP-9/TIMP-1 ratios of SSPE patients were significantly higher than the controls ($p < 0.001$ and $p = 0.005$, respectively). There were no significant differences in CSF TIMP-1 levels between the SSPE patients and controls ($p = 0.116$). There were also no significant correlations between CSF MMP-9 and TIMP-1 levels in SSPE patients. Furthermore, no significant differences in the CSF MMP-9 and TIMP-1 levels or MMP-9/TIMP-1 ratios were noted between the SSPE patients with Jabbour stage II and III (Fig. 2).

Discussion

We have previously reported serum MMP-9 and TIMP-1 levels in SSPE.[23] Serum MMP-9 levels and MMP-9/TIMP-1 ratios of SSPE patients were significantly higher than the control. Serum MMP-9 levels and MMP-9/TIMP-1 ratios of SSPE patients with Jabbour stage III were significantly higher than those with Jabbour stage II. In the brain of SSPE patients, CD4+ T lymphocytes, CD8+ T lymphocytes, and CD20+ B lymphocytes showed infiltration, especially in the perivascular regions.[25] These findings suggest that the immunocompetent cells in the blood invade the brain in SSPE patients. MMP-9 is a member of this family, which is capable of degrading collagen IV, a major component of the basement membrane of the cerebral endothelium and promotes the migration of cells through tissue or across the blood–brain–barrier (BBB).[26] Therefore, our previous study may indicate the dysfunction of the BBB in SSPE. We suggested that immunocompetent peripheral blood cells can easily invade the CNS through the BBB at high serum MMP-9 levels and MMP-9/TIMP-1 ratios in SSPE.

We newly investigated CSF MMP-9 and TIMP-1 levels in SSPE patients. Our present data were similar to the above report, with respect to the serum study. In bacterial meningitis, CSF MMP-9 is elevated and is associated with brain damage.[27–29] With regard to the pathogenesis of bacterial meningitis, the potential of MMPs to activate cytokines is intriguing.[30] Tumor necrosis factor-α (TNF-α) converting enzyme, a metalloproteinase closely related to MMPs, cleaves cell-associated TNF-α to its soluble form.[31] TNF-α is a strong stimulus for the release and activation of MMPs in the brain.[32] In bacterial meningitis, MMPs may contribute to the development of brain injury by both their proteolytic activity on the extracellular matrix and their ability to increase the levels of TNF-α.[29] We previously reported that the CSF level of soluble TNF receptor 1, which reflects the true biological activity of TNF-α,[33–35] was elevated in a boy with SSPE.[36] Moreover, several previous studies have demonstrated that TNF-α was expressed in the brain of SSPE patients.[25,37,38] Our results suggest that the CSF levels of MMP-9 may indicate the degree of inflammatory damage associated with cytokines, especially TNF-α, in SSPE. However, we could not determine a specific index indicating whether or not MMP-9 is produced in the CNS.[39] Therefore, further study is required to clarify this point. There were no significant differences in the CSF MMP-9 or TIMP-1 levels between the SSPE patients with Jabbour stage II and III in the present study, so the clinical severity could not be explained by only the CSF MMP-9 or TIMP-1 levels.

In summary, MMP-9 levels and MMP-9/TIMP-1 ratios were elevated in the CSF of patients with SSPE. It is possible that high MMP-9 levels in the CSF indicate brain inflammation and damage in SSPE. In SSPE, the MMP-9 level in serum may be an indicator of dysfunction of the BBB, and, in the CSF, of inflammatory damage to the brain.

Acknowledgements

We thank all the children, their parents, Dr. Charles S. Mgone, Dr. Joyce M. Mgone, and the staff of the Papua New Guinea Institute of Medical Research and Goroka Base General Hospital who were involved in the present study. This study was supported by grants from the Ministry of Health, Labour and Welfare (the Prion disease and Slow Virus Infection Research Committee), Japan.

References

1. Lucas KM, Sanders RC, Rongap A, Rongap T, Pinai S, Alpers MP. Subacute sclerosing panencephalitis (SSPE) in Papua New Guinea: a high incidence in young children. *Epidemiol Infect* 1992;108:547–53.
2. Takasu T, Mgone JM, Mgone CS, Miki K, Komase K, Namae H, et al. A continuing high incidence of subacute sclerosing panencephalitis (SSPE) in the Eastern Highlands of Papua New Guinea. *Epidemiol Infect* 2003;131:887–98.
3. CDC. Subacute sclerosing panencephalitis surveillance – United States. *MMWR Morb Mortal Wkly Rep* 1982;31:585–8.
4. Dyken PR. Subacute sclerosing panencephalitis. current status. *Neurol Clin* 1985;3:179–96.
5. Editorial SSPE in the developing world. *Lancet* 1990;336:600.
6. Chandler S, Miller KM, Clements JM, Lury J, Corkill D, Anthony DC, et al. Matrix metalloproteinases, tumor necrosis factor and multiple sclerosis: an overview. *J Neuroimmunol* 1997;72:155–61.
7. Welgus HG, Campbell EJ, Cury JD, Eisen AZ, Senior RM, Wilhelm SM, et al. Neutral metalloproteinases produced by human mononuclear phagocytes. enzyme profile, regulation, and expression during cellular development. *J Clin Invest* 1990;186:1496–502.
8. Chakraborti S, Mandal M, Das S, Mandal A, Chakraborti T. Regulation of matrix metalloproteinases: an overview. *Mol Cell Biochem* 2003;253:269–85.
9. Leppert D, Waubant E, Galardy R, Bunnett NW, Hauser SL. T cell gelatinases mediate basement membrane transmigration in vitro. *J Immunol* 1995;154:4379–89.
10. Rosenberg GA, Dencoff JE, Correa Jr N, Reiners M, Ford CC. Effect of steroids on CSF matrix metalloproteinases in multiple sclerosis: relation to blood–brain barrier injury. *Neurology* 1996;46:1626–32.
11. Chandler S, Coates R, Gearing A, Lury J, Wells G, Bone E. Matrix metalloproteinases degrade myelin basic protein. *Neurosci Lett* 1995;201:223–6.
12. Hartung HP, Kieseier BC. The role of matrix metalloproteinases in autoimmune damage to the central and peripheral nervous system. *J Neuroimmunol* 2000;107:140–7.
13. Newman TA, Woolley ST, Hughes PM, Sibson NR, Anthony DC, Perry VH. T-cell- and macrophage-mediated axon damage in the absence of a CNS-specific immune response: involvement of metalloproteinases. *Brain* 2001;124:2203–14.
14. Murphy G, Knäuper V. Relating matrix metalloproteinase structure to function: why the "hemopexin" domain? *Matrix Biol* 1997;15:511–8.
15. Lacraz S, Nicod LP, Chicheportiche R, Welgus HG, Dayer JM. IL-10 inhibits metalloproteinase and stimulates TIMP-1 production in human mononuclear phagocytes. *J Clin Invest* 1995;96:2304–10.

16. Waubant E, Goodkin DE, Gee L, Bacchetti P, Sloan R, Stewart T, et al. Serum MMP-9 and TIMP-1 levels are related to MRI activity in relapsing multiple sclerosis. *Neurology* 1999;**53**: 1397–401.
17. Rosenberg GA. Matrix metalloproteinases biomarkers in multiple sclerosis. *Lancet* 2005;**365**:1291–3.
18. Ribatti D, Marimpietri D, Pastorino F, Brignole C, Nico B, Vacca A, et al. Angiogenesis in neuroblastoma. *Ann N Y Acad Sci* 2004;**1028**:133–42.
19. Lee JM, Yin K, Hsin I, Chen S, Fryer JD, Holtzman DM, et al. Matrix metalloproteinase-9 in cerebral-amyloid-angiopathy-related hemorrhage. *J Neurol Sci* 2005;**229-230**:249–54.
20. Ichiyama T, Kajimoto M, Suenaga N, Maeba S, Matsubara T, Furukawa S. Serum levels of matrix metalloproteinase-9 and its tissue inhibitor (TIMP-1) in acute disseminated encephalomyelitis. *J Neuroimmunol* 2006;**172**:182–6.
21. Ichiyama T, Morishima T, Kajimoto M, Matsushige T, Matsubara T, Furukawa S. Serum levels of matrix metalloproteinase-9 and tissue inhibitors of metalloproteinases 1 in influenza-associated encephalopathy. *Pediatr Infect Dis J* 2007;**26**: 542–4.
22. Suenaga N, Ichiyama T, Kubota M, Isumi H, Tohyama J, Furukawa S. Roles of matrix metalloproteinase-9 and tissue inhibitors of metalloproteinases 1 in acute encephalopathy following prolonged febrile seizures. *J Neurol Sci* 2008;**266**: 126–30.
23. Ichiyama T, Siba P, Suarkia D, Takasu T, Miki K, Kira R, et al. Serum levels of matrix metalloproteinase-9 and tissue inhibitors of metalloproteinases 1 in subacute sclerosing panencephalitis. *J Neurol Sci* 2007;**252**:45–8.
24. Jabbour JT, Duenas DA, Modlin J. SSPE: clinical staging, course, and frequency, 1975. *Arch Neurol* 1975;**32**:493–4.
25. Anlar B, Söylemezoğlu F, Aysun S, Köse G, Belen D, Yalaz K. Tissue inflammatory response in subacute sclerosing panencephalitis (SSPE). *J Child Neurol* 2001;**16**:895–900.
26. Lukes A, Mun-Bryce S, Lukes M, Rosenberg GA. Extracellular matrix degradation by metalloproteinases and central nervous system diseases. *Mol Neurobiol* 1999;**19**:267–84.
27. Meli DN, Christen S, Leib SL. Matrix metalloproteinase-9 in pneumococcal meningitis: activation via an oxidative pathway. *J Infect Dis* 2003;**187**:1411–5.
28. Leib SL, Kim YS, Chow LL, Sheldon RA, Täuber MG. Reactive oxygen intermediates contribute to necrotic and apoptotic neuronal injury in an infant rat model of bacterial meningitis due to group B streptococci. *J Clin Invest* 1996;**98**:2632–9.
29. Leib SL, Clements JM, Lindberg RL, Heimgartner C, Loeffler JM, Pfister LA, et al. Inhibition of matrix metalloproteinases and tumour necrosis factor alpha converting enzyme as adjuvant therapy in pneumococcal meningitis. *Brain* 2001; **124**:1734–42.
30. Leib SL, Leppert D, Clements J, Täuber MG. Matrix metalloproteinases contribute to brain damage in experimental pneumococcal meningitis. *Infect Immun* 2000;**68**:615–20.
31. Solorzano CC, Ksontini R, Pruitt JH, Auffenberg T, Tannahill C, Galardy RE, et al. A matrix metalloproteinase inhibitor prevents processing of tumor necrosis factor α (TNF α) and abrogates endotoxin-induced lethality. *Shock* 1997;**7**:427–31.
32. Rosenberg GA, Estrada EY, Dencoff JE, Stetler-Stevenson WG. Tumor necrosis factor-α-induced gelatinase B causes delayed opening of the blood-brain barrier: an expanded therapeutic window. *Brain Res* 1995;**703**:151–5.
33. Duncombe AS, Brenner MK. Is circulating tumor necrosis factor bioactive? *N Engl J Med* 1988;**319**:1227.
34. Seckinger P, Issaz S, Dayer JM. A human inhibitor of tumor necrosis factor α. *J Exp Med* 1988;**167**:1511–6.
35. Engelmann H, Novick D, Wallach D. Two tumor necrosis factor-binding proteins purified from human urine; evidence for immunological cross-reactivity with cell surface tumor necrosis factor receptors. *J Biol Chem* 1990;**265**:1531–6.
36. Ichiyama T, Hayashi T, Furukawa S. Subacute sclerosing panencephalitis. *Neurology* 1997;**48**:1142–3.
37. Hofman FM, Hinton DR, Baemayr J, Weil M, Merrill JE. Lymphokines and immunoregulatory molecules in subacute sclerosing panencephalitis. *Clin Immunol Immunopathol* 1991;**58**: 331–42.
38. Nagano I, Nakamura S, Yoshioka M, Onodera J, Kogure K, Itoyama Y. Expression of cytokines in brain lesions in subacute sclerosing panencephalitis. *Neurology* 1994;**44**:710–5.
39. Liuzzi GM, Trojano M, Fanelli M, Avolio C, Fasano A, Livrea P, et al. Intrathecal synthesis of matrix metalloproteinase-9 in patients with multiple sclerosis: implication for pathogenesis. *Mult Scler* 2002;**8**:222–8.

Cytokine 44 (2008) 149–153

Contents lists available at ScienceDirect

Cytokine

journal homepage: www.elsevier.com/locate/issn/10434666

Cerebrospinal fluid levels of cytokines in non-herpetic acute limbic encephalitis: Comparison with herpes simplex encephalitis

Takashi Ichiyama [a,*], Hiroshi Shoji [b], Yukitoshi Takahashi [c], Takeshi Matsushige [a], Madoka Kajimoto [a], Takashi Inuzuka [d], Susumu Furukawa [a]

[a] Department of Pediatrics, Yamaguchi University Graduate School of Medicine, 1-1-1 Minamikogushi, Ube, Yamaguchi 755-8505, Japan
[b] International University of Health and Welfare, Ohkawa, Japan
[c] National Epilepsy Center, Shizuoka Institute of Epilepsy and Neurological Disorders, Shizuoka, Japan
[d] Department of Neurology and Geriatrics, Gifu University Graduate School of Medicine, Gifu, Japan

ARTICLE INFO

Article history:
Received 26 May 2008
Received in revised form 20 June 2008
Accepted 14 July 2008

Keywords:
Cerebrospinal fluid
Herpes simplex encephalitis
Interferon-γ
Non-herpetic acute limbic encephalitis
Soluble tumor necrosis factor receptor 1

ABSTRACT

Background: Recently, non-herpetic acute limbic encephalitis (NHALE) was identified as a new subgroup of limbic encephalitis. The immunological pathophysiology of NHALE is still unclear. *Methods:* We measured the concentrations of interferon-γ (IFN-γ), tumor necrosis factor-α (TNF-α), interleukin-2 (IL-2), IL-4, IL-6, IL-10, and soluble TNF receptor 1 (sTNFR1) in the cerebrospinal fluid (CSF) of 15 patients with NHALE and 13 with herpes simplex encephalitis (HSE) by cytometric bead array or ELISA. *Results:* The CSF concentrations of IL-6 in patients with NHALE and IFN-γ, IL-6, IL-10, and sTNFR1 in HSE patients were significantly higher than those of controls ($p < 0.001$, $p = 0.004$, $p < 0.001$, $p = 0.018$, and $p < 0.001$, respectively). There were significant correlations among CSF IL-6, IL-10, and sTNFR1 levels in HSE patients. The CSF concentrations of IFN-γ and sTNFR1 levels of patients with HSE were significantly higher than those with NHALE ($p = 0.001$ and $p = 0.002$, respectively). *Conclusions:* CSF cytokine levels in NHALE were relatively low compared with those in HSE. These results may be related to the favorable prognosis of NHALE.

1. Introduction

In Japan, non-herpetic acute limbic encephalitis (NHALE) was identified as a new subgroup of limbic encephalitis [1–3]. The clinical picture of NHALE is similar to that of herpes simplex encephalitis (HSE). However, the disease is not caused by herpes simplex virus (HSV) infection or a paraneoplastic disease process. Many previously reported patients with NHALE had a rather favorable neurological prognosis compared to those with HSE [2,4]. There have been a few reports on the autopsy cases with NHALE [4,5]. These reports demonstrated that there were neuronal loss and severe gliosis with inflammatory cell infiltrations in the hippocampus and amygdala. The pathogenesis of NHALE is still unclear.

To investigate the immunological pathogenesis of NHALE, we determined the cerebrospinal fluid (CSF) concentrations of interferon-γ (IFN-γ), tumor necrosis factor-α (TNF-α), interleukin-2 (IL-2), IL-4, IL-6, IL-10, and soluble TNF receptor 1 (sTNFR1) as cytokines related to inflammation in patients with NHALE and HSE.

2. Patients and methods

Informed consent was obtained from the families of the patients and controls enrolled in this study.

2.1. NHALE

CSF samples were obtained from 15 patients with NHALE (five males and 10 females, aged from 12 to 82 years; median, 35 years) admitted to Yamaguchi University Hospital and seven collaborating research hospitals from July 1999 to February 2008 (Tables 1 and 2). The criteria for the diagnosis of NHALE were: (1) acute or subacute onset neurological disorder with limbic-associated symptoms, such as amnesia, delirium, panic, anxiety, excitation, etc., (2) negative HSV DNA in CSF by the nested polymerase chain reaction (PCR) and negative HSV antibodies in CSF determined by the enzyme-linked immunosorbent assay (ELISA), (3) lesions of the temporal lobe, especially hippocampi and amygdalae, on magnetic resonance imaging (MRI) (Fig. 1), (4) absence of malignancy, (5) no bacteria or fungi in CSF culture, and (6) the exclusion of all other neurological, vascular, metabolic, endocrine, toxic, and drug-induced disorders. CSF samples obtained during the acute stage were stored at −70 °C.

* Corresponding author. Fax: +81 836 22 2257.
E-mail address: ichiyama@yamaguchi-u.ac.jp (T. Ichiyama).

1043-4666/$ - see front matter © 2008 Elsevier Ltd. All rights reserved.
doi:10.1016/j.cyto.2008.07.002

2.2. HSE

CSF samples were obtained from 13 patients with HSE (eight males and five females, aged from 13 to 76 years; median, 61 years) admitted to Yamaguchi University Hospital and two collaborating research hospitals from October 2000 to December 2005 (Table 1). The diagnosis was based on the demonstration of HSV DNA in the CSF by nested PCR. CSF samples during acute stage were stored at −70 °C.

2.3. Control subjects

The control subjects for the CSF levels of the cytokines were 19 afebrile and non-infectious patients with neurological disorders, such as epilepsy, dementia, etc. (11 males and eight females, aged from 13 to 79 years; median, 55 years), as shown in Table 1. CSF samples were obtained from them on routine analysis and they all had normal CSF cell counts.

2.4. Clinical data

The clinical data including age, gender, clinical symptoms on admission, CSF findings at the time of specimen collection, MRI findings during the acute stage, and clinical outcomes in patients with NHALE and HSE were investigated. The outcomes were defined as follows: (1) normal resolution, (2) mild sequelae, (3) severe sequelae necessitating help with daily life activities, and (4) death [6].

2.5. Determination of cytokine concentrations

The concentrations of CSF IFN-γ, TNF-α, IL-2, IL-4, IL-6, and IL-10 were measured with a cytometric bead array (CBA) kit (BD PharMingen, San Diego, CA, USA) according to the manufacturer's manual, as previously described [7–9], with modification of the data analysis using GraphPad Prism software (GraphPad Prism Software, San Diego, CA, USA). Briefly, each series of beads exhibiting discrete fluorescence intensities is coated with a monoclonal antibody against a single cytokine, and a mixture of six series of beads can detect six cytokines in one sample. A secondary phycoerythrin-conjugated monoclonal antibody stains the beads proportionally to the amount of bound cytokine. After fluorescence intensity calibration and electronic color compensation procedures, standard and test samples were analyzed with a FACScan flow cytometer equipped with CellQuest software (BD PharMingen). The lower detection limits for IFN-γ, TNF-α, IL-2, IL-4, IL-6, and IL-10 were 7.1, 2.8, 2.6, 2.6, 2.5, and 2.8 pg/ml, respectively.

The CSF concentrations of sTNFR1 were determined with a sTNFR1 ELISA kit (Bender Medsystems, Vienna, Austria), as described previously [10]. The lower detection limit for sTNFR1 was 0.05 ng/ml.

2.6. Statistical analysis

All data were log transformed to obtain an approximately normal distribution. The differences in the results between groups were analyzed with a t-test and the χ^2 test, and those with a p-value of less than 0.05 were considered significant. Correlations were analyzed using Pearson's coefficient correlation. Analyses and calculations were performed using SPSS-12.0 (SPSS, Inc., Chicago, IL, USA).

3. Results

3.1. Clinical characteristics

Clinical data of patients with NHALE are shown in Tables 1 and 2. There were no significant differences in age or gender among patients with NHALE and HSE and controls (median age, 35, 61, and 55 years, respectively). The CSF cell counts of patients with NHALE were lower than those with HSE ($p = 0.015$, 9/μl vs. 32/μl as a median). The CSF protein levels of patients with NHALE were less than those with HSE ($p = 0.003$, 33 vs. 50 mg/dl as a median). Of the 15 patients with NHALE, 9 (67%) had mild sequelae and 6 (33%) survived without sequelae. Of the 13 patients with HSE, 1 (8%) died and 12 (92%) experienced disability (54% had severe and 38% had mild sequelae).

Table 1
Clinical data of patients with NHALE, HSE, and controls

	NHALE $N = 15$	HSE $N = 13$	Control subjects $N = 19$
Age (median, range)	35 yr, 11–82 yr	61 yr, 13–76 yr	55 yr, 13–79 yr
Sex (male: female)	5:10	8:5	11:8
Comorbid conditions	–	–	Epilepsy, 9; dementia, 5; psychosis, 4; Tic, 1
Prognosis	Normal, 6; mild sequelae, 9	Mild sequelae, 5; severe sequelae, 7; death, 1	–

NHALE, non-herpetic acute limbic encephalitis; HSE, herpes simplex encephalitis.

Table 2
Clinical characteristics of the 15 patients with non-herpetic acute limbic encephalitis

No./age/gender	Main symptoms on admission	Lesions on MRI	CSF findings		Neurological prognosis
			Cell (μl)	Protein (mg/dl)	
1/34 yr/M	Amnesia, delirium	Bilateral temporal lobes	12	39	Normal
2/73 yr/F	Somnolence, convulsion	Bilateral temporal lobes	32	24	Normal
3/35 yr/M	Amnesia, convulsion	Bilateral temporal lobes	9	39	Mild amnesia
4/11 yr/M	Convulsion, delirium	Right temporal lobe	187	33	Intellectual impairment
5/18 yr/F	Convulsion	Bilateral temporal lobes	39	31	Normal
6/49 yr/F	Amnesia, convulsion	Bilateral temporal lobes	42	50	Amnesia, psychopathy
7/31 yr/F	Convulsion	Bilateral temporal lobes	0	27	Epilepsy
8/47 yr/F	Insomnia, convulsion	Bilateral temporal lobes	9	47	Normal
9/82 yr/F	Amnesia, fugue	Bilateral temporal lobes	1	39	Amnesia
10/67 yr/M	Convulsion, delirium	Bilateral temporal lobes	1	35	Amnesia
11/75 yr/F	Convulsion, enuresis	Bilateral temporal lobes	0	32	Amnesia, psychopathy
12/51 yr/M	Amnesia, convulsion	Bilateral temporal lobes	0	28	Amnesia
13/14 yr/F	Panic	Left temporal lobe	121	27	Normal
14/19 yr/F	Excitation, convulsion	Bilateral temporal lobes	8	48	Intellectual impairment, epilepsy
15/12 yr/F	Anxiety, insomnia	Bilateral temporal lobes	14	25	Normal

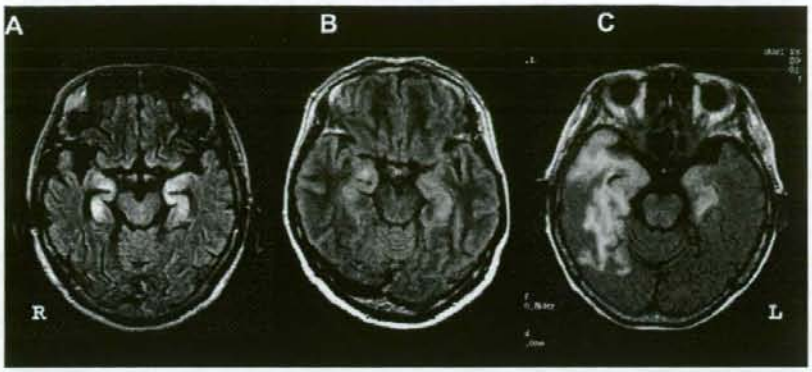

Fig. 1. FLAIR MRI of Patient 2 (A), Patient 6 (B), and Patient 9 (C) demonstrated high signal intensity lesions in the bilateral temporal lobes.

3.2. CSF concentrations of cytokines

In patients with NHALE, the CSF concentrations of IL-6 were significantly higher than those of controls ($p < 0.001$), but those of IFN-γ, TNF-α, IL-2, IL-4, IL-10, or sTNFR1 were not (Fig. 2).

In patients with HSE, the CSF concentrations of IFN-γ, IL-6, IL-10, and sTNFR1 were significantly higher than those of controls ($p = 0.004$, $p < 0.001$, $p = 0.018$, and $p < 0.001$, respectively), but those of TNF-α, IL-2, or IL-4 were not (Fig. 2). There were significant correlations among CSF IL-6, IL-10, and sTNFR1 levels in HSE patients (IL-6 and IL-10, $p = 0.008$; IL-6 and sTNFR1, $p < 0.001$; IL-10 and sTNFR1, $p = 0.030$) (Fig. 3).

The CSF concentrations of IFN-γ and sTNFR1 levels of patients with HSE were significantly higher than those with NHALE ($p = 0.001$, and $p = 0.002$, respectively) (Fig. 2).

4. Discussion

Main lesions in NHALE were in the bilateral temporal lobes, especially the hippocampus and amygdala, similar to those in HSE. However, HSV DNA or anti-HSV antibodies were not detected in the CSF of patients with NHALE. Previous reports on autopsy cases of NHALE revealed that HSV-1 or -2 were not detected in the brain [4,5]. Therefore, NHALE has been identified as a new type of encephalitis, especially in Japan [1–4]. Several autoantibodies, including those against the *N*-methyl-D-aspartate glutamate receptor and voltage-gated potassium channel, were detected in patients with NHALE [4,11–14]. Moreover, patients with limbic encephalitis associated with autoimmune disease, including Hashimoto's disease, Sjögren's syndrome, and systemic lupus erythematosus, have been reported [15–17]. These previous studies suggest that NHALE is immune-mediated encephalitis.

The clinical outcomes of patients with NHALE were relatively favorable compared with those with HSE. Moreover, CSF cell counts and protein concentrations of patients with NHALE were significantly less and lower than those with HSE, suggesting that inflammation in the CNS in NHALE is milder than that in HSE. In this study, we demonstrated CSF cytokine profiles of NHALE compared with HSE. In patients with NHALE, the CSF concentrations of IL-6 were significantly higher than those of controls, but those of IFN-γ, TNF-α, IL-2, IL-4, IL-10, or sTNFR1 were not. IL-6 is well-known as a cytokine that plays important roles in inflammatory re-

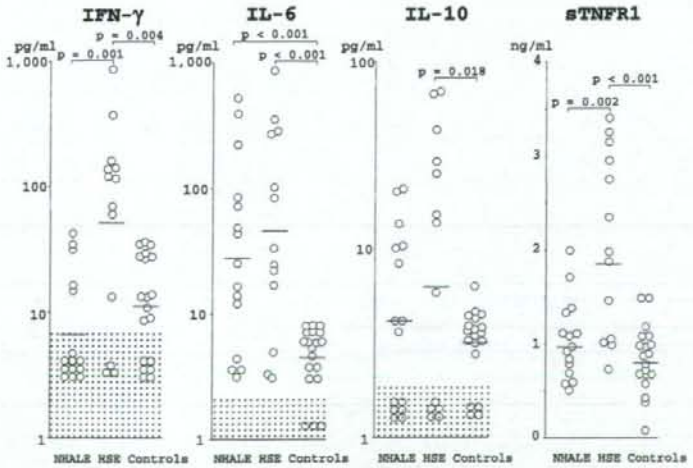

Fig. 2. The CSF concentrations of IFN-γ, IL-6, IL-10, and sTNFR1 in patients with NHALE, HSE, and controls. Horizontal lines indicate geometric means. Shaded areas indicate values below the detection limits.

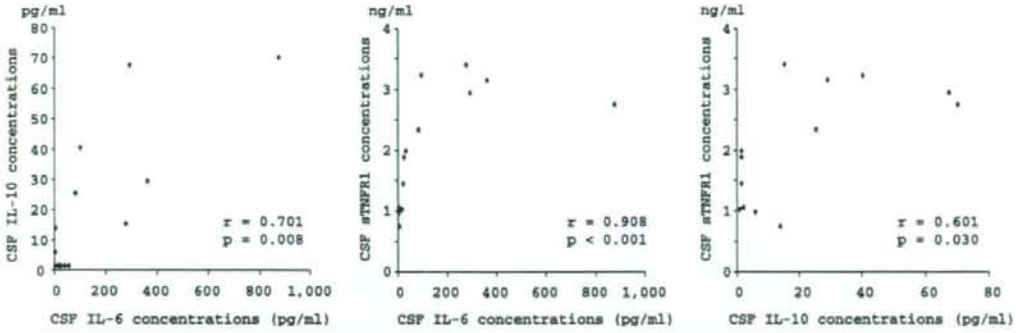

Fig. 3. The relationship among CSF IL-6, IL-10, and sTNFR1 concentrations in patients with HSE. r, Pearson's coefficient.

sponses [18,19]. Our results suggested that NHALE involves mild inflammation modified by IL-6 in the central nervous system (CNS). IFN-γ, which is produced by NK cells and $CD8^+$ and Th1 type $CD4^+$ T lymphocytes, plays an important role in host defense against viral infection, and inhibits viral replication [20]. We previously demonstrated that CSF IFN-γ levels were elevated in CNS disorders due to direct viral invasion, such as viral meningitis and HSE [2,21,22], but not in immune-mediated CNS disorders, such as acute disseminated encephalomyelitis, influenza-associated encephalopathy, acute encephalopathy following prolonged febrile seizures, and hemolytic uremic syndrome with encephalopathy [23–26]. Taking our findings into consideration, NHALE without elevated IFN-γ levels in the CSF in this study is not caused by direct viral infection.

In patients with HSE, the CSF concentrations of IFN-γ, IL-6, IL-10, and sTNFR1 were significantly higher than those with controls. Our present data that CSF IFN-γ levels were elevated in HSE were consistent with a previous study [2]. There were significant correlations among CSF IL-6, IL-10, and sTNFR1 levels in HSE patients. In addition, CSF sTNFR1 levels in HSE were significantly higher than those in NHALE. TNF-α increases blood–brain vascular permeability, injures vascular endothelial cells, and induces the necrosis of myelin and oligodendrocytes [29–31]. Previous studies have suggested that TNF-α mediates the pathogenesis of acute encephalitis/encephalopathy [23,32–35]. It is believed that sTNFR reflects the true biological activity of TNF-α [36–38]. CSF sTNFR1 levels are related to the neurological prognosis in bacterial meningitis and acute encephalopathy/encephalitis [10,33]. CSF sTNFR1 levels may reflect the neurological outcome in HSE. IL-10 as an anti-inflammatory cytokine decreases the production of IL-1, IL-6, and TNF-α induced by an endotoxin or bacteria [27,28]. Therefore we suggest that IL-10 is induced in the CNS to modulate pro-inflammatory cytokine-mediated inflammation in the CNS of patients with HSE. Patients with HSE showed elevated pro-inflammatory and anti-inflammatory cytokines in the CSF, suggesting that there was severe inflammation in the CNS of these patients.

In conclusion, the CSF concentrations of IL-6 in patients with NHALE and IFN-γ, IL-6, IL-10, and sTNFR1 in HSE patients were significantly higher than those in controls. Patients with HSE had many elevated cytokines in the CSF, but those with NHALE showed only an elevated CSF level of IL-6. These findings may be related to the fact that the clinical outcome of NHALE is relatively favorable compared with that of HSE.

Acknowledgments

This study was supported by grants from the Ministry of Health, Labour and Welfare, Japan. We thank Drs. A. Nishiguchi (Tachikawa Sougo Hospital), H. Hino (Graduate School of Medical Sciences, Kumamoto University), Y. Miyazaki (Toho University School of Medicine), J. Kira (Graduate School of Medical Sciences, Kyushu University), and S. Tsuji (School of Medicine, University of Occupational and Environmental Health) for contributing to this study.

References

[1] Kusuhara T, Shoji H, Kaji M, Ayabe M, Hino H. Non-herpetic acute limbic encephalitis. Rinsho Shinkeigaku 1994;34:1083–8 [In Japanese].
[2] Asaoka K, Shoji H, Nishizaka S, Ayabe M, Abe T, Ohori N, et al. Non-herpetic acute limbic encephalitis: cerebrospinal fluid cytokines and magnetic resonance imaging findings. Intern Med 2004;43:42–8.
[3] Shoji H, Asaoka K, Ayabe M, Ichiyama T, Sakai K. Non-herpetic acute limbic encephalitis: a new subgroup of limbic encephalitis? Intern Med 2004;43:348.
[4] Mochizuki Y, Mizutani T, Isozaki E, Ohtake T, Takahashi Y. Acute limbic encephalitis: a new entity? Neurosci Lett 2006;394:5–8.
[5] Maki T, Kokubo Y, Nishida S, Suzuki H, Kuzuhara S. An autopsy case with non-herpetic acute limbic encephalitis (NHALE). Neuropathology, in press.
[6] Morishima T, Togashi T, Yokota S, Okuno Y, Miyazaki C, Tashiro M, et al. Collaborative study group on influenza-associated encephalopathy in Japan. Encephalitis and encephalopathy associated with an influenza epidemic in Japan. Clin Infect Dis 2002;35:512–7.
[7] Chen R, Lowe L, Wilson JD, Crowther E, Tzeggai K, Bishop JE, et al. Simultaneous quantification of six human cytokines in a single sample using microparticle-based flow cytometric technology. Clin Chem 1999;45:1693–4.
[8] Cook EB, Stahl JL, Lowe L, Chen R, Morgan E, Wilson J, et al. Simultaneous measurement of six cytokines in a single sample of human tears using microparticle-based flow cytometry: allergics vs. non-allergics. J Immunol Methods 2001;254:109–18.
[9] Metelitsa LS, Naidenko OV, Kant A, Wu HW, Loza MJ, Perussia B, et al. Human NKT cells mediate antitumor cytotoxicity directly by recognizing target cell CD1d with bound ligand or indirectly by producing IL-2 to activate NK cells. J Immunol 2001;167:3114–22.
[10] Ichiyama T, Hayashi T, Furukawa S. Cerebrospinal fluid concentrations of soluble tumor necrosis factor receptor in bacterial and aseptic meningitis. Neurology 1996;46:837–8.
[11] Kimura A, Sakurai T, Suzuki Y, Hayashi Y, Hozumi I, Watanabe O, et al. Autoantibodies against glutamate receptor ε_2-subunit detected in a subgroup of patients with reversible autoimmune limbic encephalitis. Eur Neurol 2007;58:152–8.
[12] Vincent A, Buckley C, Schott JM, Baker I, Dewar BK, Detert N, et al. Potassium channel antibody-associated encephalopathy: a potentially immunotherapy-responsive form of limbic encephalitis. Brain 2004;127:701–12.
[13] Fauser S, Talazko J, Wagner K, Ziyeh S, Jarius S, Vincent A, et al. FDG-PET and MRI in potassium channel antibody-associated non-paraneoplastic limbic encephalitis: correlation with clinical course and neuropsychology. Acta Neurol Scand 2005;111:338–43.
[14] Iranzo A, Graus F, Clover L, Morera J, Bruna J, Vilar C, et al. Rapid eye movement sleep behavior disorder and potassium channel antibody-associated limbic encephalitis. Ann Neurol 2006;59:178–81.
[15] Ide T, Iizuka T, Suzuki N. Limbic encephalitis associated with autoimmune diseases. Shinkei Naika 2003;59:31–7 [In Japanese].
[16] Mocellin R, Walterfang M, Velakoulis D. Hashimoto's encephalopathy: epidemiology, pathogenesis and management. CNS Drugs 2007;21:799–811.
[17] Stübgen JP. Nervous system lupus mimics limbic encephalitis. Lupus 1998;7:557–60.
[18] Heinrich PC, Castell JV, Andus T. Interleukin-6 and the acute phase response. Biochem J 1990;265:621–36.
[19] Tracey KJ, Vlassara H, Cerami A. Cachectin/tumor necrosis factor. Lancet 1989;1:1122–6.

[20] Samuel CE. Antiviral actions of interferon. Interferon-regulated cellular proteins and their surprisingly selective antiviral activities. Virology 1991;183:1–11.
[21] Matsubara T, Matsuoka T, Katayama K, Yoshitomi T, Nishikawa M, Ichiyama T, et al. Mononuclear cells and cytokines in the cerebrospinal fluid of echovirus 30 meningitis patients. Scand J Infect Dis 2000;32:471–4.
[22] Ichiyama T, Maeba S, Suenaga N, Saito K, Matsubara T, Furukawa S. Analysis of cytokine levels in cerebrospinal fluid in mumps meningitis: comparison with echovirus type 30 meningitis. Cytokine 2005;30:243–7.
[23] Ichiyama T, Shoji H, Kato M, Sawaishi Y, Ozawa H, Matsubara T, et al. Cerebrospinal fluid levels of cytokines and soluble tumor necrosis factor receptor in acute disseminated encephalomyelitis. Eur J Pediatr 2002;161:133–7.
[24] Ichiyama T, Morishima T, Isumi H, Matsufuji H, Matubara T, Furukawa S. Analysis of cytokine levels and NF-κB activation in peripheral blood mononuclear cells in influenza virus-associated encephalopathy. Cytokine 2004;27:31–7.
[25] Ichiyama T, Suenaga N, Kajimoto M, Tohyama J, Isumi H, Kubota M, et al. Serum and CSF levels of cytokines in acute encephalopathy following prolonged febrile seizures. Brain Dev 2008;30:47–52.
[26] Shiraishi M, Ichiyama T, Matsushige T, Iwaki T, Iyoda K, Fukuda K, et al. Soluble tumor necrosis factor receptor 1 and tissue inhibitors of metalloproteinases-1 in hemolytic uremic syndrome with encephalopathy. J Neuroimmunol 2008;196:147–52.
[27] Howard M, Muchamuel T, Andrade S, Menon S. Interleukin 10 protects mice from lethal endotoxemia. J Exp Med 1993;177:1205–8.
[28] Paris MM, Hickey SM, Trujillo M, Ahmed A, Olsen K, McCracken Jr GH. The effect of interleukin-10 on meningeal inflammation in experimental bacterial meningitis. J Infect Dis 1997;176:1239–46.
[29] Mustafa MM, Lebel MH, Ramilo O, Olsen KD, Reisch JS, Beutler B, et al. Correlation of interleukin-1β and cachectin concentrations in cerebrospinal fluid and outcome from bacterial meningitis. J Pediatr 1989;115:208–13.
[30] Salmaj KW, Raine CS. Tumor necrosis factor mediates myelin and oligodendrocyte damage in vitro. Ann Neurol 1988;23:339–46.
[31] Sato N, Goto T, Haranaka K, Satomi N, Nariuchi H, Mano-Hirano Y, et al. Actions of tumor necrosis factor on cultured vascular endothelial cells: morphologic modulation, growth inhibition, and cytotoxicity. J Natl Cancer Inst 1986;76:1113–21.
[32] Aurelius E, Andersson B, Forsgren M, Sköldenberg B, Strannegård O. Cytokines and other markers of intrathecal immune response in patients with herpes simplex encephalitis. J Infect Dis 1994;170:678–81.
[33] Ichiyama T, Hayashi T, Nishikawa M, Furukawa S. Cerebrospinal fluid levels of soluble tumor necrosis factor receptor in acute encephalitis. J Neurol 1996;243:457–60.
[34] Ichiyama T, Nishikawa M, Yoshitomi T, Hayashi T, Furukawa S. Tumor necrosis factor-α, interleukin-1β and interleukin-6 in cerebrospinal fluid from children with prolonged febrile seizures. Comparison with acute encephalitis/encephalopathy. Neurology 1998;50:407–11.
[35] Ichiyama T, Isumi H, Ozawa H, Matsubara T, Morishima T, Furukawa S. Cerebrospinal fluid and serum levels of cytokines and soluble tumor necrosis factor receptor in influenza virus-associated encephalopathy. Scand J Infect Dis 2003;35:59–61.
[36] Duncombe AS, Brenner MK. Is circulating tumor necrosis factor bioactive? N Engl J Med 1988;319:1227.
[37] Seckinger P, Issaz S, Dayer JM. A human inhibitor of tumor necrosis factor α. J Exp Med 1988;167:1511–6.
[38] Engelmann H, Novick D, Wallach D. Two tumor necrosis factor-binding proteins purified from human urine; evidence for immunological cross-reactivity with cell surface tumor necrosis factor receptor. J Biol Chem 1990;265:1531–6.

Rheumatol Int (2008) 28:1277–1280
DOI 10.1007/s00296-008-0611-y

CASE REPORT

Reversible stenosis of large cerebral arteries in a patient with combined Sjögren's syndrome and neuromyelitis optica spectrum disorder

Yuichiro Ii · Akihiro Shindo · Ryogen Sasaki · Yutaka Naito · Keiko Tanaka · Shigeki Kuzuhara

Received: 7 February 2008 / Accepted: 4 May 2008 / Published online: 21 May 2008

Abstract We report a 49-year-old woman with neuromyelitis optica (NMO) spectrum disorder coexisting with Sjögren's syndrome (SS). She presented with acute brainstem symptoms and transverse myelitis. Brain MRI showed focal high signal intensity lesions in the hypothalamus and the pontine tegmentum on T2-weighted and FLAIR images. MRA revealed stenotic changes of the bilateral middle cerebral artery (MCA), posterior cerebral arteries (PCA) and basilar artery (BA). Spinal MRI revealed hyperintense lesions within the cord extending from the T4 to the T6 level on the T2-weighted image. The patient fulfilled the clinical criteria of primary SS. In addition, anti-AQP4 antibody which is highly specific for NMO was detected in the serum at the acute phase. The patient excellently responded to IVIg while methylprednisolon pulse therapy was not effective. Follow-up MRA displayed complete resolution of the stenosis of the MCA, PCA and BA.

Y. Ii (✉) · A. Shindo · R. Sasaki · Y. Naito · S. Kuzuhara
Department of Neurology,
Mie University Graduate School of Medicine,
2-174, Edobashi, Tsu, Mie 514-8507, Japan
e-mail: ii-y@clin.medic.mie-u.ac.jp

K. Tanaka
Department of Neurology,
Brain Research Institute, Niigata University, Niigata, Japan

S. Kuzuhara
Department of Neurology,
National Center of Neurology and Psychiatry Musashi Hospital,
Tokyo, Japan

Keywords Neuromyelitis optica · Sjögren's syndrome · Anti SS-A antibody · Anti-aquaporin 4 antibody · MRA

Introduction

Neuromyelitis optica (NMO) is an idiopathic inflammatory demyelinating disorder of the central nervous system (CNS) characterized by severe optic neuritis (ON) and myelitis [1]. Recently, the serum autoantibody NMO-IgG was reported as a biomarker of NMO [2]. NMO-IgG binds selectively to mercurial-insensitive water channel protein aquaporin 4 (AQP4), which is concentrated in astrocytic foot processes at the blood–brain barrier [3]. NMO-IgG is detected not only in typical NMO but also in "NMO spectrum disorder" such as recurrent isolated myelitis and ON, clinically symptomatic or subclinical brain lesions and coexsisting with autoimmune disorders including SLE and Sjögren's syndrome (SS) [4]. SS accompanied by NMO have rarely been reported [5–8], but the definitive causal relationship between NMO and SS remains to be clarified.

Recent MRI studies [9] have revealed evidence of brain lesions in 60% of patients who fulfill the 1999 criteria of [1] for the diagnosis of NMO other than brain MRI findings. Subsequently, Pittock et al. [10] described the NMO-characteristic brain lesions on MRI localized to the sites of high AQP4 expression, which include hypothalamus, periventricular areas, especially of the third and forth ventricles. Recently, anti-AQP4 antibody detection system was established [11, 12]. This autoantibody is an equally sensitive and highly specific biomarker for NMO as NMO-IgG [11, 13].

We report here a patient with combined SS and NMO spectrum disorder who showed reversible transient stenosis of the large cerebral arteries.

Case report

A 49-year-old woman presented with a 3 days history of progressive diplopia, disturbance of gait and bradyuria after headache, nausea and vomitting. She visited a general practitioner 4 days after the onset. Brain MR imaging showed focal high signal intensity lesions in the hypothalamus and the pontine tegmentum on T2-weighted and fluid-attenuated inversion recovery (FLAIR) images. She was referred to our hospital next day. The patient had experienced xerostomia since young but not been closely examined. There was no family history of autoimmune diseases. Neurological examination on admission (5 days after the onset) showed MLF syndrome in the right side, ataxic gait and bradyuria. Cerebrospinal fluid (CSF) analysis revealed a mild lymphocytic pleocytosis (24 cells/mm^3), normal level of protein and glucose (44 and 81 mg/dl). The oligoclonal IgG band was negative. Myelin basic protein was elevated at 1,010 pg/ml (normal 0–102 pg/ml). A tentative diagnosis of multiple scrlosis was made, and pulse therapy with intravenous 1,000 mg of methylprednisolone was done for 4 days, which was followed by 1 mg/kg day^{-1} oral prednisolone. Although corticosteroid administration, her ocular movement deteriorated from unilateral to bilateral MLF syndrome and paraparesis with bilateral extensor plantar responses, loss of sensation in the legs and urinary retention progressed.

The laboratory tests showed positive rheumatoid factor, anti-Ro (SS-A) and anti-La (SS-B) antibodies. Other immunologic tests including antinuclear antibody, anti-DNA antibody, lupus anticoagulant, antineutrophil cytoplasmic antibody, anticardiolipin immunoglobulin M and immunoglobulin G antibodies were normal. She had a positive Schirmer's test with 5 mm of tearing. A salivary gland biopsy revealed inflammatory changes. The laboratory data fulfilled the criteria of primary SS [14].

Cranial MR imaging on 7 days after the onset (Fig. 1a–c) showed focal high signal intensity lesions in the hypothalamus and the pontine tegmentum on T2-weighted and FLAIR images. These lesions were not enhanced on T1-weighted image with gadolinium administration. MR angiography (MRA) on the same day revealed severe narrowing of the bilateral proximal portion of the posterior cerebral arteries (PCA) and basilar artery (BA) with multiple segmental stenosis and mild narrowing of the right middle cerebral artery (MCA) (Fig. 2a, b). Spinal MRI on 15 days after the onset revealed hyperintense lesion within the cord extending from the T4 to the T6 level on T2-weighted sequences, which was slightly enhanced with gadolinium administration. She was treated with methylprednisolone pulse therapy which was followed by oral prednisolone (1 mg/kg day^{-1}), but disturbance of gait deteriorated and loss of sensation extended below the T5 level. Intravenous immunoglobulin (IVIg) therapy (0.4 g/kg day^{-1} for 5 days) was initiated 14 days after the onset. The symptoms began to gradually improve in the middle of IVIg therapy. She became to be able to walk without support. Ocular movement, sensory disturbances and urinary retention also improved slowly.

Cranial MRI on T2-weighted and FLAIR images examined 18 days after the onset (Fig. 1d–f) showed high signal intensity in the occipital lobes bilaterally without presentation with any clinical symptoms. MRA on the same day (Fig. 2c, d) revealed slight improvement of the stenotic change of the bilateral PCA and BA and severe narrowing of the bilateral MCA. Therapy with oral prednisolone was continued. She was discharged 33 days after the onset with mild paresthesia in the legs and dysuria.

We received the report that anti-AQP 4 antibody of the serum at the acute stage was positive after her discharge, and made the final diagnosis of NMO spectrum disorder [15] coexsisting with SS. The abnormal findings in the occipital lobes completely disappeared on the follow-up cranial MRI (Fig. 1g–i). The lesions in the hypothalamus and the pontine tegmentum still remained. MRA taken 3 months after the onset (Fig. 2e, f) displayed complete resolution of stenosis of the bilateral MCA, PCA and BA.

Discussion

We described a case of NMO spectrum disorder in a patient with SS. Pittock et al. [16] and Weinshenker et al. [17] have identified the NMO-like disorder in some patients with SLE and SS. Clinical or serological markers of SLE and SS were found in approximately half of NMO patients [16, 17] while the markers of patients with NMO rarely fulfilled the diagnostic criteria for SS [6–8, 16]. In the present case, it seems that the patient has had Sjögren's syndrome as an underlying disease because she had experienced xerostomia since young. Widespread B cell immune response as SS of the patient may be activated to produce anti-AQP4 antibody, which is highly specific for NMO [11, 13].

Lesions on MRI in the hypothalamus and the pontine tegmentum are the characteristic brain lesions in NMO [10], and similar lesions were shown in the present case. Brain lesions in NMO on MRI are often asymptomatic, and resolve rapidly in some patients [9, 10]. These lesions may reflect a transient functional impairment of the normal astrocytic control of the water flux that follows the initial binding of IgG to AQP4 [18]. Transient asymptomatic bilateral occipital lesions observed in the present case may have been produced by the same pathogenesis.

The most interesting feature of the present case was the reversible transient stenosis of the large cerebral arteries demonstrated by MRA. Similar condition was reported in

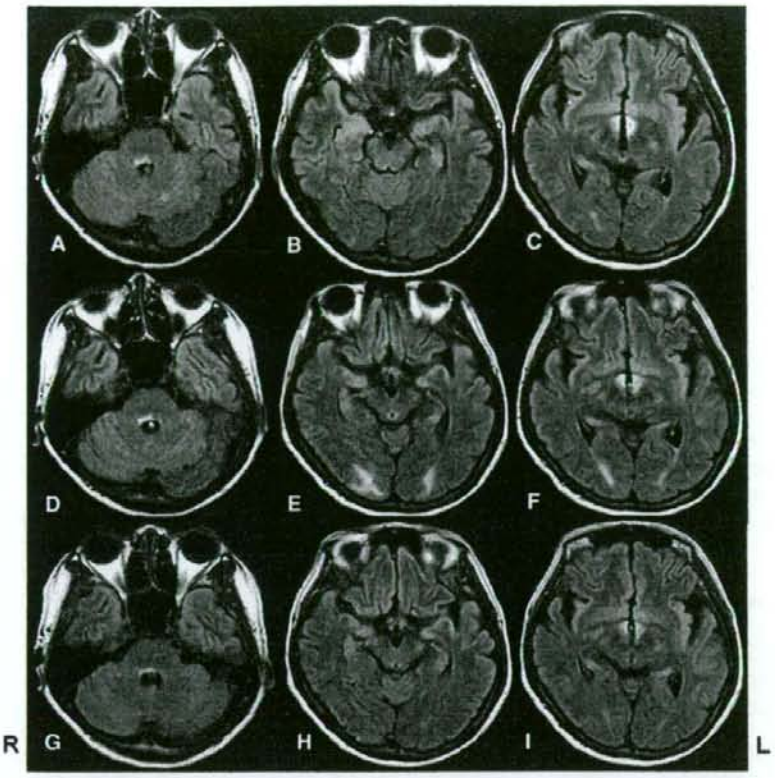

Fig. 1 Cranial MRI on FLAIR images. High signal intensity lesions in the hypothalamus and the pontine tegmentum are observed on 7 days after the onset (**a–c**). New lesions in the bilateral occipital lobes on 18 days (**d–f**). The occipital lesions are gone on 39 days while the lesions in the hypothalamus and the pontine tegmentum remain (**g–i**)

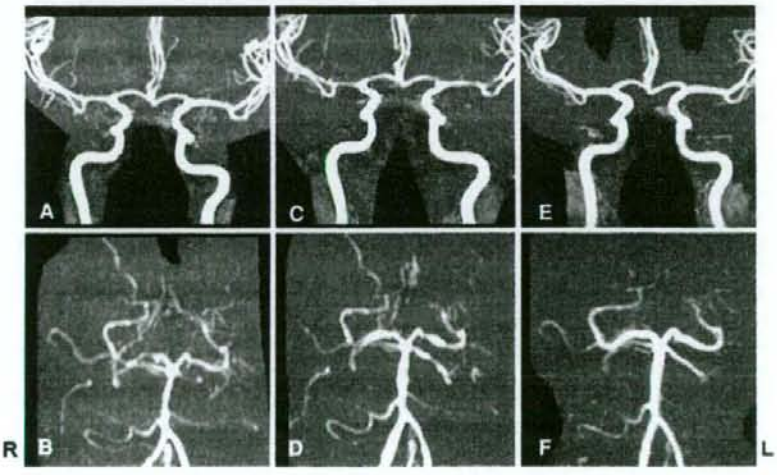

Fig. 2 Serial MR angiographies. Mild narrowing of right middle cerebral artery (*MCA*), and multiple segmental stenosis of the bilateral posterior cerebral arteries (*PCA*) and basilar artery (*BA*) on 7 days after the onset (**a, b**). Slight improvement of stenosis of PCA and BA and progression of narrowing of bilateral MCA on 18 days (**c, d**). Complete resolution of the stenotic changes 3 months after the onset (**e, f**)

some autoimmune diseases, and autoimmune cerebral vasculitis or vasculopathy was suggested [19–21]. A few cases of SS presenting with stenosis of large cerebral arteries were reported [22, 23]. Alexander et al. [22] suggested a possible relationship between positive anti-SS-A antibody and vasculitis. In the present case the pathogenesis of the reversible cerebral arterial stenosis is unclear. B cell-mediated autoimmune condition based on NMO and SS [24, 25]

may have induced the autoimmune inflammatory reversible arteriopathy.

The treatment currently recommended for NMO and NMO spectrum disorder at the acute phase is intravenous corticosteroid plus an immunosuppressive agent [4]. Plasma exchange is also recommended for the cases unresponsive to administration of corticosteroid [26, 27]. The present patient eventually failed to respond to methylprednisolon pulse therapy but dramatically reacted to IVIg. In NMO and NMO spectrum disorder, IVIg may be a good option for the treatment at the acute stage.

References

1. Wingerchuk DM, Hogancamp WF, O'Brien PC, Weinshenker BG (1999) The clinical course of neuromyelitis optica (Devic's syndrome). Neurology 53:1107–1114
2. Lennon VA, Wingerchuk DM, Kryzer TJ, Pittock SJ, Lucchinetti CF, Fujihara K, Nakashima I, Weinshenker G (2004) A serum autoantibody marker of neuromyelitis optica: distinction from multiple sclerosis. Lancet 364:2106–2112
3. Lennon VA, Kryzer TJ, Pittock SJ, Verkman AS, Hinson SR (2005) IgG marker of optic-spinal multiple sclerosis binds to the aquaporin-4 water channel. J Exp Med 202:473–477
4. Jacob A, Matiello M, Wingerchuk DM, Lucchinetti CF, Pittock SJ, Weinshenker BG (2007) Neuromyelitis optica: changing concepts. J Neuroimmunol 187:126–138
5. Alexander EL, Ranzenbach MR, Kumar AJ, Kozachuk WE, Rosenbaum AE, Patronas N, Harley JB, Reichlin M (1994) Anti-Ro(SSA) autoantibodies in central nervous system disease associated with Sjögren's syndrome (CNS-SS): clinical, neuroimaging, and angiographic correlates. Neurology 44:899–908
6. Harada T, Ohashi T, Miyagishi R, Fukuda H, Yoshida K, Tagawa Y, Matsuda H (1995) Optic neuropathy and acute transverse myelopathy in primary Sjögren's syndrome. Jpn J Ophthalmol 39:162–165
7. Mochizuki A, Hayashi A, Hisahara S, Shoji S (2000) Steroid-responsive Devic's variant in Sjögren's syndrome. Neurology 54:1391–1392
8. Gökçay F, Çelebisoy N, Gökçay A, Kabasakal Y, Öder G (2007) Primary Sjögren's syndrome presenting as neuromyelitis optica. Pediatr Neurol 36:58–60
9. Pittock SJ, Lennon VA, Krecke K, Wingerchuk DM, Lucchinetti CF, Weinshenker BG (2006) Brain abnormalities in patients with neuromyelitis optica. Arch Neurol 63:390–396
10. Pittock SJ, Weinshenker BG, Lucchinetti CF, Wingerchuk DM, Corboy JR, Lennon VA (2006) Neuromyelitis optica brain lesions localized at sites of high aquaporin 4 expression. Arch Neurol 63:964–968
11. Takahashi T, Fujihara K, Nakashima I, Misu T, Miyazawa I, Nakamura M, Watanabe S, Ishii N, Itoyama Y (2006) Establishment of a new sensitive assay for anti-human aquaporin-4 antibody in neuromyelitis optica. Tohoku J Exp Med 210:307–313
12. Tanaka K, Tani T, Tanaka M, Saida T, Idezuka J, Yamazaki M, Tsujita M, Nakada T, Sakimura K, Nishizawa M (2007) Anti-aquaporin 4 antibody in selected Japanese multiple sclerosis patients with long spinal cord lesions. Mult Scler 13:850–855
13. Takahashi T, Fujihara K, Nakashima I, Misu T, Miyazawa I, Nakamura M, Watanabe S, Shiga Y, Kanaoka C, Fujimori J, Sato S, Itoyama Y (2007) Anti-aquaporin-4 antibody is involved in the pathogenesis of NMO: a study on antibody titre. Brain 130:1235–1243
14. Vitali C, Bombardieri S, Jonsson R, Moutsopoulos HM, Alexander EL, Carsons SE, Daniels TE, Fox PC, Fox RI, Kassan SS, Pillemer SR, Talal N, Weisman MH, the European Study Group on Classification Criteria for Sjögren's syndrome (2002) Classification criteria for Sjögren's syndrome: a revised version of the European criteria proposed by the American-European Consensus Group. Ann Rheum Dis 61:554–558
15. Wingerchuk DM, Lennon VA, Pittock SJ, Lucchinetti CF, Weinshenker BG (2006) Revised diagnostic criteria for neuromyelitis optica. Neurology 66:1485–1489
16. Pittock SJ, Lennon VA, Wingerchuk DM, Homburger HA, Lucchinetti CF, Weinshenker BG (2006) The prevalence of non-organ-specific autoantibodies and NMO-IgG in neuromyelitis optica (NMO) and related disorders [abstract]. Neurology 66(Suppl 2):A307
17. Weinshenker B, De Seze J, Vemersch P, Pittock SJ, Lennon VA (2006) The relationship between neuromyelitis optica and systemic autoimmune disease [abstract]. Neurology 66(Suppl 2):A380
18. Compston A (2007) Complexity and heterogeneity in demyelinating disease. Brain 130:1178–1180
19. Pedersen RC, Rerson DA (1998) Cerebral vasculitis in an adolescent with juvenile rheumatoid arthritis. Pediatr Neurol 19:69–73
20. Kondo K, Yamawaki T, Nagatsuka K, Miyashita K, Naritomi H (2003) Reversible stenosis of major cerebral arteries demonstrated by MRA in thrombotic thrombocytopenic purpura. J Neurol 250:995–997
21. Utku U, Asil T, Çelik Y, Tucer D (2004) Reversible MR angiographic findings in a patient with autoimmune Graves disease. AJNR 25:1541–1543
22. Alexander GE, Provost TT, Stevens MB, Alexander EL (1981) Sjögren's syndrome: central nervous system manifestations. Neurology 31:1391–1396
23. Nagahiro S, Mantani A, Yamada K, Ushio Y (1996) Multiple cerebral arterial occlusions in a young patient with Sjögren's syndrome: case report. Neurosurgery 38:592–595
24. Lucchinetti CF, Mandler RN, McGavern D, Bruck W, Gleich G, Ransohoff RM, Trebst C, Weinshenker B, Wingerchuk D, Parisi JE, Lassmann H (2002) A role for humoral mechanisms in the pathogenesis of Devic's neuromyelitis optica. Brain 125:1450–1461
25. Delaleu N, Jonsson R, Koller MM (2005) Sjögren's syndrome. Eur J Oral Sci 113:101–113
26. Keegan M, Pineda AA, McClelland RL, Darby CH, Rodriguez M, Weinshenker BG (2002) Plasma exchange for severe attacks of CNS demyelination: predictors of response. Neurology 58:143–146
27. Watanabe S, Nakashima I, Misu T, Miyazawa I, Shiga Y, Fujihara K, Itoyama Y (2007) Therapeutic efficacy of plasma exchange in NMO-IgG-positive patients with neuromyelitis optica. Mult Scler 13:128–132

Brief Communications

NMDA- and β-Amyloid$_{1-42}$-Induced Neurotoxicity Is Attenuated in Serine Racemase Knock-Out Mice

Ran Inoue,[1] Kenji Hashimoto,[2] Tomomi Harai,[1] and Hisashi Mori[1]

[1]Department of Molecular Neuroscience, Graduate School of Medicine and Pharmaceutical Sciences, University of Toyama, Toyama 930-0194, Japan, and [2]Division of Clinical Neuroscience, Center for Forensic Mental Health, Chiba University, Chiba 260-8670, Japan

D-Serine is detected in the brain and acts as a coagonist at the "glycine-site" of the NMDA-type glutamate receptor. Although D-serine can be directly produced from L-serine by serine racemase (SR), the relative contribution of SR in D-serine formation *in vivo* is not known. Pathological roles of brain D-serine mediating NMDA receptor overactivation are suggested in studies using *in vitro* culture systems. However, we have recently demonstrated the differential SR protein expression *in vivo* and in culture. Here, we reported an ~90% decrease in forebrain D-serine content in SR knock-out (KO) mice. We also found a reduced neurotoxicity induced by NMDA- and Aβ$_{1-42}$-peptide injections into the forebrain in SR KO mice. These results suggest that SR is the major enzyme for D-serine production in the brain, D-serine is the predominant endogenous coagonist of the NMDA receptor in the forebrain, and D-serine may be involved in controlling the extent of NMDA receptor-mediated neurotoxic insults observed in disorders including Alzheimer's disease. The control of SR activity and D-serine level in the brain may lead to a novel strategy for neuroprotection against various neurodegenerative diseases.

Key words: D-Serine; serine racemase; NMDA receptor; neurotoxicity; Alzheimer's disease; gene knock-out mice

Introduction

The mammalian brain contains high levels of D-serine, which acts as a coagonist at the "glycine-site" of the NMDA-type glutamate receptor (GluR). The origin of brain D-serine was speculative before the discovery of serine racemase (SR) in the mammalian brain (Wolosker et al., 1999a,b). SR catalyzes racemization and dehydration of serine (De Miranda et al., 2002). Enzymatic characterizations of purified SR suggest that the catalytic constant (k_{cat}) for D-serine in the racemization by mouse SR is ~1/400 of prokaryotic racemase, and the k_{cat}/K_m of SR in the dehydration of L-serine is higher than those in the racemization for serine (Yoshimura and Goto, 2008). The activity of SR is decreased by glycine at a physiological concentration (Dunlop and Neidle, 2005) and by modification with *S*-nitrosylation (Mustafa et al., 2007). Thus, the contribution of SR to D-serine production in the brain should be evaluated *in vivo*.

NMDA-type GluR plays key roles in neural network formation during development, synaptic plasticity, and neurodegenerative disorders including Alzheimer's disease (AD) (Bliss and Collingridge, 1993; Komuro and Rakic, 1993; Lancelot and Beal, 1998). In cultured hippocampal neurons, degradation of D-serine by treatment with D-amino acid oxidase (DAAO) decreases NMDA-receptor-mediated currents (Mothet et al., 2000) and diminishes long-term potentiation in cultured hippocampal neurons (Yang et al., 2003). In the forebrain, there are sufficient amounts of free D-serine and glycine for activation of the NMDA receptor (Hashimoto et al., 1995). D-Serine and glycine may control the extent of NMDA receptor-mediated neurotoxicity. A study using D-serine deaminase demonstrated that D-serine, but not glycine, mediates NMDA receptor-elicited cell death in organotypic hippocampal slices (Shleper et al., 2005). These reports using culture systems strongly support the hypothesis that D-serine is a major endogenous ligand for the NMDA receptor. However, we have recently reported the differential expression of the SR protein in the brain and in culture (Miya et al., 2008). Thus, the relative importance of two coagonists, D-serine and glycine, in NMDA receptor activation in the brain remains unclear.

AD is a major neurodegenerative disorder in which the excitotoxic effect of D-serine may be involved. The β-amyloid peptide (Aβ) is proposed as the main pathological factor for AD. Some extent of calcium-mediated neurotoxicity exerted by Aβ can be mediated by the NMDA receptor (Suh and Checler, 2002). DAAO protects neurons against Aβ-induced Ca^{2+} overload and neurotoxicity, providing evidence that D-serine may be a death signal induced by Aβ (Wu et al., 2004). As mentioned above, most of the studies on D-serine with respect to the regulation of various brain functions have been limited in culture systems and enzymatic degradation of D-serine. To investigate the roles of SR and endogenous D-serine *in vivo*, we have recently established SR knock-out (KO) mice (Miya et al., 2008). In the present study, we found that SR KO mice showed ~90% decrease in brain D-serine content and attenuation of NMDA- and Aβ-elicited neurotoxicity.

Received Oct. 17, 2008; revised Nov. 21, 2008; accepted Nov. 25, 2008.

This work was supported by grants from Ministry of Education, Culture, Sports, Science, and Technology of Japan (Grant No. 507-16047210 and 507-18053008). We thank Prof. Masahiko Watanabe for providing anti-NMDAR subunit antibodies, Prof. Masakiyo Sasahara for the use of histochemical equipments and advice, Ms. Takako Matsushima for paraffin block preparation, and Ms. Yuko Fujita for HPLC measurement of amino acids.

Correspondence should be addressed to Dr. Hisashi Mori, Department of Molecular Neuroscience, Graduate School of Medicine and Pharmaceutical Sciences, University of Toyama, Toyama 930-0194, Japan. E-mail: hmori@med.u-toyama.ac.jp.

DOI:10.1523/JNEUROSCI.5034-08.2008

 0270-6474/08/2814486-06$15.00/0

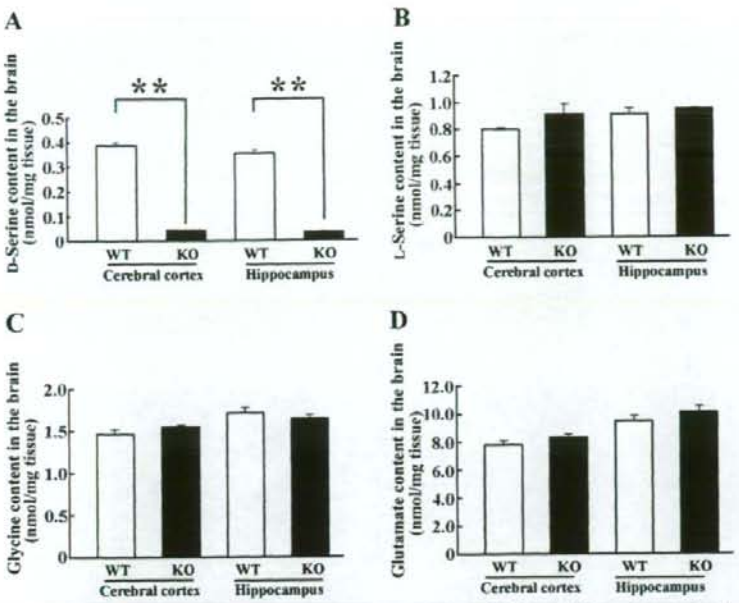

Figure 1. Serine racemase is a major enzyme for D-serine production in the brain. ***A***, HPLC revealed that D-serine contents in the cerebral cortex and hippocampus of serine racemase knock-out (SR KO, KO) mice were ~10-fold lower than those of WT mice. ***B–D***, The contents of L-serine, glycine, and glutamate in the cerebral cortex and hippocampus of SR-KO mice were comparable with those of WT mice. The data represent mean ± SEM from six mice. $^{**}p < 0.001$; two-tailed Student's *t* test.

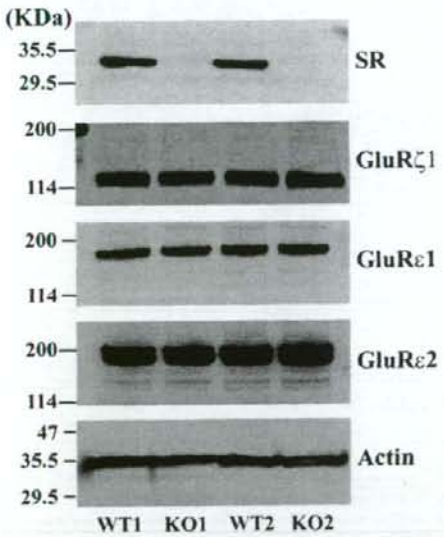

Figure 2. Expression level of NMDA receptor subunits in SR KO mice is comparable with that in WT mice. Western blot analyses of the forebrain proteins of two WT and SR KO (KO) mice by use of anti-SR, anti-GluRζ1, anti-GluRε1, anti-GluRε2, and anti-actin antibodies. The positions of protein size markers are indicated on the left side. The SR protein was detected in WT mice, but not in SR KO mice. There were no marked differences in the expression levels of the three NMDA receptor subunits between WT and SR KO mice.

Materials and Methods

Mice. Animal care and experimental protocols were performed in accordance with the Guidelines for the Care and Use of Laboratory Animals at University of Toyama. The SR KO mice were generated from C57BL/6-derived embryonic stem cells transfected with the gene-targeting vector containing C57BL/6 mouse genomic DNA, and were expanded by crossing with C57BL/6 mice (Miya et al., 2008). Generation and genotyping of the SR KO and wild-type (WT) control mice with pure C57BL/6 genetic background have been reported previously (Miya et al., 2008). The WT and SR KO mice at the age of 2–3 months were used for analyses in a genotype blind manner.

High-performance liquid chromatography analysis. Mice were starved overnight. Measurement of D-serine, L-serine, glycine, and glutamate levels in the brain homogenate was performed according to established methods using a column-switching high-performance liquid chromatography (HPLC) system (Shimadzu) (Fukushima et al. 2004). A 20 μl aliquot sample was processed and analyzed as described previously (Kanahara et al., 2008).

Antibodies. Goat polyclonal anti-SR antibody, rabbit polyclonal anti-actin antibody, HRP-conjugated donkey anti-goat IgG, and HRP-conjugated donkey anti-mouse IgG were purchased from Santa Cruz Biotechnology. Rabbit polyclonal anti-GluRε1 and anti-GluRε2 antibodies (Watanabe et al., 1998) were provided by Dr. Masahiko Watanabe (Hokkaido University, Sapporo, Japan). Mouse monoclonal anti-GluRζ1 was purchased from BD Biosciences Pharmigen. HRP-conjugated goat anti-rabbit IgG was purchased from Bio-Rad.

Western blotting. The WT and SR KO mice were deeply anesthetized with pentobarbital sodium [100 mg/kg body weight (b.w.)] by intraperitoneal injection, perfused transcardially with ice-cold PBS, pH 7.4. Brains were quickly removed and forebrain tissue was homogenized in ice-cold mammalian protein extraction reagent (Pierce). Protein extracts (100 μg) was subjected to SDS-PAGE and transferred onto a polyvinylidene difluoride membrane. After blocking with a solution containing 5% skim milk in PBS, membranes were incubated with primary antibodies of anti-SR (1:500), anti-GluRε1 (NR2A) (0.5 μg/ml), anti-GluRε2 (NR2B) (0.5 μg/ml), and anti-GluRζ1 (NR1) (0.5 μg/ml) overnight at 4°C, then with HRP-conjugated secondary antibody for 1 h. Protein bands were detected using the ECL chemiluminescence detection system (GE Healthcare).

Aβ preparation. Human $A\beta_{1-42}$ peptide and control human $A\beta_{42-1}$ peptide (Peptide Institute) were dissolved in 2 mM DMSO at a concentration of 4 μg/μl and were stored at −80°C until use. The $A\beta_{1-42}$ or $A\beta_{42-1}$ peptide was diluted with same volume of 200 mM DMSO immediately before Aβ injection.

Intracerebral drug administration. The WT and SR KO mice were deeply anesthetized with 3.6% chloral hydrate in PBS by intraperitoneal injection (10 ml/kg b.w.) and mounted in a stereotaxic frame. The skull was exposed and 0.5 μl of 100 mM NMDA or 100 mM NMDA combined with 100 mM D-serine (Tocris) was injected into right parietal cortex at a site, 1.6 mm caudal to bregma, 1 mm right from the midline, and 0.8 mm below the dural surface. Mice were decapitated 24 h after the injection under the deep anesthesia with pentobarbital sodium.

For Aβ injection, 1 μl of $A\beta_{1-42}$ or $A\beta_{42-1}$ peptide at the concentration 2 μg/μl was injected into right hippocampus at a site, 2 mm caudal to bregma, 1.5 mm right from the midline, and 1.9 mm below the dural surface. Dizocilpine maleate (MK-801, 0.8 mg/kg b.w.) was intraperitoneally administered 2 h before $A\beta_{1-42}$ injection. Mice were decapitated 48 h after the injection under the deep anesthesia with pentobarbital sodium.

Histology. The WT and SR KO mice were deeply anesthetized with pentobarbital sodium by intraperitoneal injection and perfused transcardially with ice-cold PBS followed by 4% paraformaldehyde. Brains were

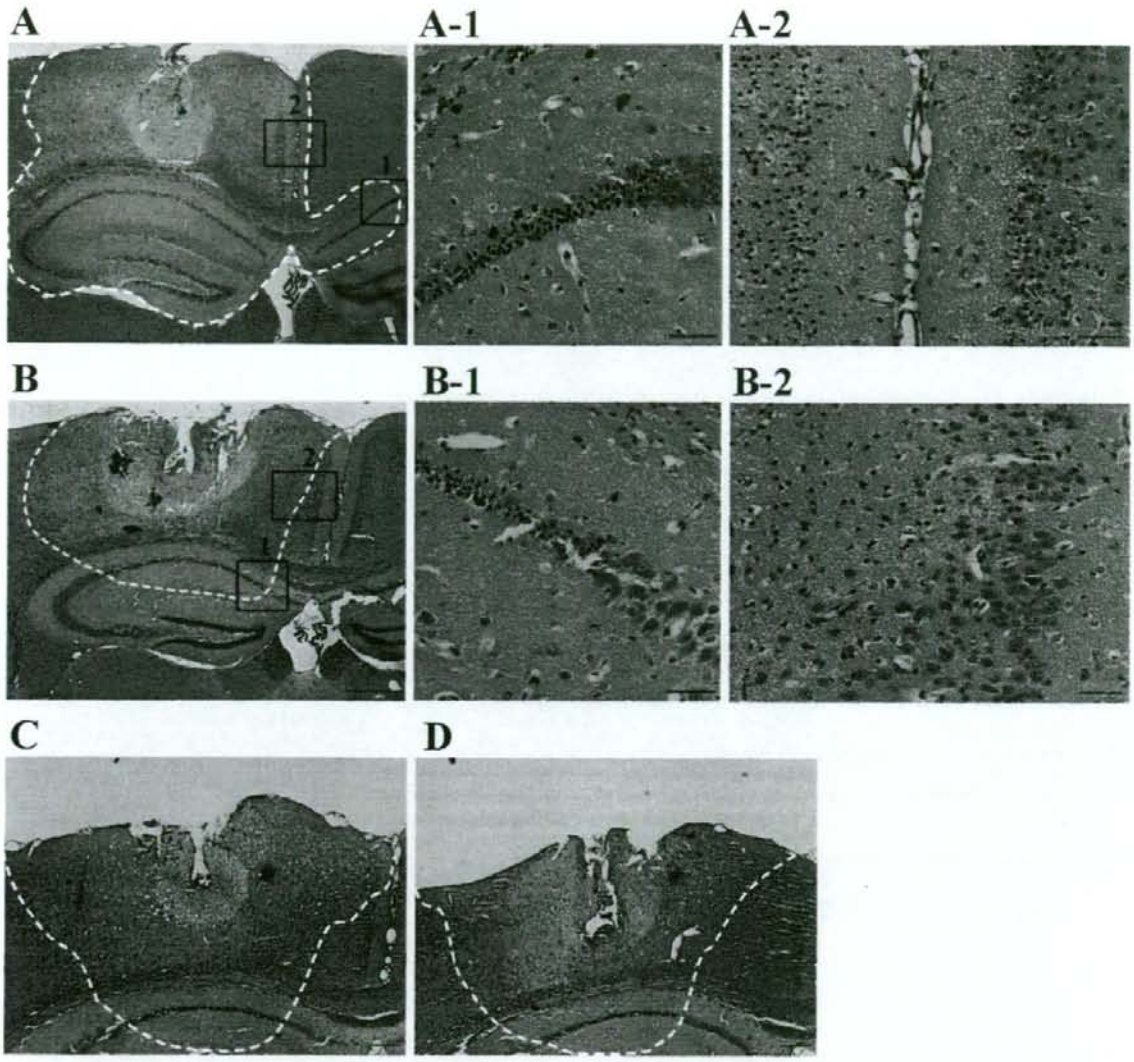

Figure 3. NMDA-induced neuronal damage is attenuated in SR KO mice. ***A***, ***B***, HE-stained brain sections of WT (***A***) and SR KO (***B***) mice 24 h after NMDA injection. ***A-1***, ***A-2***, High-magnification images corresponding to rectangles 1 and 2 in ***A***, respectively. ***B-1***, ***B-2***, High-magnification images corresponding to rectangles 1 and 2 in ***B***, respectively. ***C***, ***D***, HE-stained brain sections of WT (***C***) and SR KO (***D***) mice 24 h after coinjection of NMDA and D-serine. White dotted lines in ***A–D*** delineate the regions of neurodegeneration. Scale bars: ***A***, ***B***, 500 μm; ***A-1***, ***A-2***, ***B-1***, ***B-2***, 50 μm; ***C***, ***D***, 200 μm.

removed and fixed with same fixative for overnight. The fixed brains were then embedded in paraffin and cut into 10 μm thick coronal sections at intervals of 100 μm. These sections were glass-mounted and stained for hematoxylin/eosin (HE). Digital image of HE-stained sections were taken with an Olympus AX80 microscope (Olympus). In HE-stained brain sections, the area damaged after drug injection showed decreased stainability that probably correspond to the edematous change and cellular degeneration. In accordance with these areas, the high-magnification view revealed that the degenerated neurons were distributed with shrunken and pyknotic nuclei. Neuronal death was further confirmed in these damaged areas by the Nissl staining conducted on the adjacent sections. After these observations, the damaged areas were delineated on the digital images of HE-stained sections and were quantified using MetaMorph software (Universal Imaging). Then, the injury volume was calculated as a pile of columns, each with an evaluated area and a height of 100 μm as reported by Ishii et al. (2006).

Statistical analysis. All values are represented as mean ± SEM. Statistical significance between WT and SR KO mice was determined by two-tailed Student's *t* test. Values of $p < 0.05$ were considered significant.

Results

D-Serine content in SR KO mice brain

To examine whether SR is responsible for the production of D-serine in the brain, D-serine content was measured in the brain homogenate of SR KO and WT mice. HPLC revealed that D-serine content in the cerebral cortex and hippocampus of SR KO mice (0.043 ± 0.004 and 0.037 ± 0.001 nmol/mg tissue, respectively; $n = 6$) were ~10-fold lower than those in WT mice (0.388 ± 0.011 and 0.355 ± 0.012 nmol/mg tissue, respectively; $n = 6$) (Fig. 1*A*). In contrast, the levels of L-serine, glycine, and glutamate in the cerebral cortex of SR KO mice (0.917 ± 0.073,

Komuro H, Rakic P (1993) Modulation of neuronal migration by NMDA receptors. Science 260:95–97.

Lambert MP, Barlow AK, Chromy BA, Edwards C, Freed R, Liosatos M, Morgan TE, Rozovsky I, Trommer B, Viola KL, Wals P, Zhang C, Finch CE, Krafft GA, Klein WL (1998) Diffusible, nonfibrillar ligands derived from Abeta1–42 are potent central nervous system neurotoxins. Proc Natl Acad Sci U S A 95:6448–6453.

Lancelot E, Beal MF (1998) Glutamate toxicity in chronic neurodegenerative disease. Prog Brain Res 116:331–347.

Matsui T, Sekiguchi M, Hashimoto A, Tomita U, Nishikawa T, Wada K (1995) Functional comparison of D-serine and glycine in rodents: the effect on cloned NMDA receptors and the extracellular concentration. J Neurochem 65:454–458.

Miya K, Inoue R, Takata Y, Abe M, Natsume R, Sakimura K, Hongou K, Miyawaki T, Mori H (2008) Serine racemase is predominantly localized in neurons in mouse brain. J Comp Neurol 510:641–654.

Mothet JP, Parent AT, Wolosker H, Brady RO Jr, Linden DJ, Ferris CD, Rogawski MA, Snyder SH (2000) D-Serine is an endogenous ligand for the glycine site of the N-methyl-D-aspartate receptor. Proc Natl Acad Sci U S A 97:4926–4931.

Mustafa AK, Kumar M, Selvakumar B, Ho GP, Ehmsen JT, Barrow RK, Amzel LM, Snyder SH (2007) Nitric oxide S-nitrosylates serine racemase, mediating feedback inhibition of D-serine formation. Proc Natl Acad Sci U S A 104:2950–2955.

Price DL (1986) New perspectives on Alzheimer's disease. Annu Rev Neurosci 9:489–512.

Shleper M, Kartvelishvily E, Wolosker H (2005) D-Serine is the dominant endogenous coagonist for NMDA receptor neurotoxicity in organotypic hippocampal slices. J Neurosci 25:9413–9417.

Suh YH, Checler F (2002) Amyloid precursor protein, presenilins, and alpha-synuclein: molecular pathogenesis and pharmacological applications in Alzheimer's disease. Pharmacol Rev 54:469–525.

Watanabe M, Fukaya M, Sakimura K, Manabe T, Mishina M, Inoue Y (1998) Selective scarcity of NMDA receptor channel subunits in the stratum lucidum (mossy fibre-recipient layer) of the mouse hippocampal CA3 subfield. Eur J Neurosci 10:478–487.

Wolosker H, Sheth KN, Takahashi M, Mothet JP, Brady RO Jr, Ferris CD, Snyder SH (1999a) Purification of serine racemase: biosynthesis of the neuromodulator D-serine. Proc Natl Acad Sci U S A 96:721–725.

Wolosker H, Blackshaw S, Snyder SH (1999b) Serine racemase: a glial enzyme synthesizing D-serine to regulate glutamate-N-methyl-D-aspartate neurotransmission. Proc Natl Acad Sci U S A 96:13409–13414.

Wood PL, Hawkinson JE, Goodnough DB (1996) Formation of D-serine from L-phosphoserine in brain synaptosomes. J Neurochem 67:1485–1490.

Wu SZ, Bodles AM, Porter MM, Griffin WS, Basile AS, Barger SW (2004) Induction of serine racemase expression and D-serine release from microglia by amyloid beta-peptide. J Neuroinflammation 1:2.

Yang Y, Ge W, Chen Y, Zhang Z, Shen W, Wu C, Poo M, Duan S (2003) Contribution of astrocytes to hippocampal long-term potentiation through release of D-serine. Proc Natl Acad Sci U S A 100:15194–15199.

Yoshimura T, Goto M (2008) D-Amino acids in the brain: structure and function of pyridoxal phosphate-dependent amino acid racemases. FEBS J 275:3527–3537.

Cancer Immunity (13 November 2008) Vol. 8, p. 15
Submitted: 18 September 2008. Accepted: 27 October 2008.

CANCER
IMMUNITY
Article

Identification of the HERV-K gag antigen in prostate cancer by SEREX using autologous patient serum and its immunogenicity

Toshiaki Ishida[1,2], Yuichi Obata[3], Nobuya Ohara[4], Hirokazu Matsushita[1], Shuichiro Sato[1], Akiko Uenaka[1], Takashi Saika[5], Takako Miyamura[2], Kosuke Chayama[2], Yurika Nakamura[6], Hisashi Wada[6], Toshiharu Yamashita[7], Tsuneo Morishima[2], Lloyd J. Old[8] and Eiichi Nakayama[1]

[1]*Department of Immunology, Okayama University Graduate School of Medicine, Dentistry and Pharmaceutical Sciences, 2-5-1 Shikata-cho, Okayama 700-8558, Japan*

[2]*Department of Pediatrics, Okayama University Graduate School of Medicine, Dentistry and Pharmaceutical Sciences, 2-5-1 Shikata-cho, Okayama 700-8558, Japan*

[3]*RIKEN Bioresource Center, 3-1-1 Koyadai, Tsukuba, Ibaraki 305-0074, Japan*

[4]*Department of Pathology, Okayama University Graduate School of Medicine, Dentistry and Pharmaceutical Sciences, 2-5-1 Shikata-cho, Okayama 700-8558, Japan*

[5]*Department of Urology, Okayama University Graduate School of Medicine, Dentistry and Pharmaceutical Sciences, 2-5-1 Shikata-cho, Okayama 700-8558, Japan*

[6]*Department of Surgery, Graduate School of Medicine, Osaka University, 2-2 Yamada-oka, Suita, Osaka 565-0871, Japan*

[7]*Department of Dermatology, Sapporo Medical University School of Medicine, S1W16 Chuo-ku, Sapporo, Hokkaido 060-8543, Japan*

[8]*Ludwig Institute for Cancer Research, New York Branch at Memorial Sloan-Kettering Cancer Center, 1275 York Avenue, New York, NY 10021, USA*

Contributed by: LJ Old

The prostate cancer HERV-K gag-related NGO-Pr-54 antigen was identified by SEREX analysis using autologous patient serum. *NGO-Pr-54* mRNA was observed to be faintly expressed in normal prostate and strongly expressed in a variety of cancers, including ovarian cancer (5/8), prostate cancer (6/9), and leukemia (5/14). A phage plaque assay showed that a strong reaction was constantly observed with clone ZH042 in which the 5' end of *NGO-Pr-54* is deleted, suggesting that it contained the sequence coding for the protein product. A TI-35 mAb was produced using a recombinant protein (438 aa) deduced from the sequence of ZH042. Transfection of clone ZH042 into 293T cells resulted in the production of an approximately 50-kDa molecule visualized by Western blotting. Natural production of the molecule was confirmed in a SK-MEL-23 melanoma cell line. An indirect immunofluorescence assay showed that NGO-Pr-54 protein was expressed on the cell surface as well as in the cytoplasm. Cell surface expression was confirmed by flow cytometry using the TI-35 mAb. The antibody response against NGO-Pr-54 was observed in patients with bladder (5.1%), liver (4.1%), lung (3.4%), ovarian (5.6%), and prostate (4.2%) cancer, as well as with malignant melanoma (13.2%).

Keywords: human, prostate cancer, SEREX, HERV-K, gag, tumor antigen

Introduction

Serological recombinant cDNA expression cloning (SEREX) has been utilized for the identification of tumor antigens (1, 2). More than 2,000 antigens including cancer/testis antigens, mutational antigens, over-expressed antigens, differentiation antigens, splice-variant antigens and viral antigens have been defined by SEREX (2). Some SEREX-defined antigens, such as NY-ESO-1 (3, 4, 5), Her2/neu (6), NY-BR-1 (7), etc., have also been identified as targets of cellular immune responses.

Human endogenous retroviruses (HERVs) are genomic sequences that result from ancient retroviral infections that became fixed in the germ line DNA (8, 9) and represent approximately 8% of the human genome (10). More than twenty HERV families have been identified (11). Most HERV families are defective; however, some families still contain open reading frames (ORFs) for retroviral genes (12). HERVs contain *gag*, *pol*, and *env* genes encoding polyproteins flanked by two long terminal repeats (LTRs) (9, 13). The HERV-K family is the most conserved family. It is present as 30-50 proviral copies in the human genome (14) and has intact ORFs for the *gag*, *pol*, or *env* genes (15, 16). No expression of HERVs has been observed in most normal tissues. However, HERVs have been shown to be expressed in normal placenta (17) and brain (18, 19) from patients with multiple sclerosis. In tumors, HERV-K was shown to be expressed in teratocarcinoma (20) and HERV-E in prostate cancer (21).

In this study, the NGO-Pr-54 antigen was identified by immunoscreening of cDNA expression libraries prepared from prostate cancer specimens obtained from a patient with autologous sera. NGO-Pr-54 is homologous to HERV-K. The mRNA expression was examined in various normal tissues and in a variety of tumors from different origins. The ORF was determined and mAb was produced. Its localization on the cell surface as well as in the cytoplasm was demonstrated. The immunogenicity of NGO-Pr-54, as evidenced by the production of antibody in cancer patients, was shown by ELISA using the recombinant protein.

Figure 1

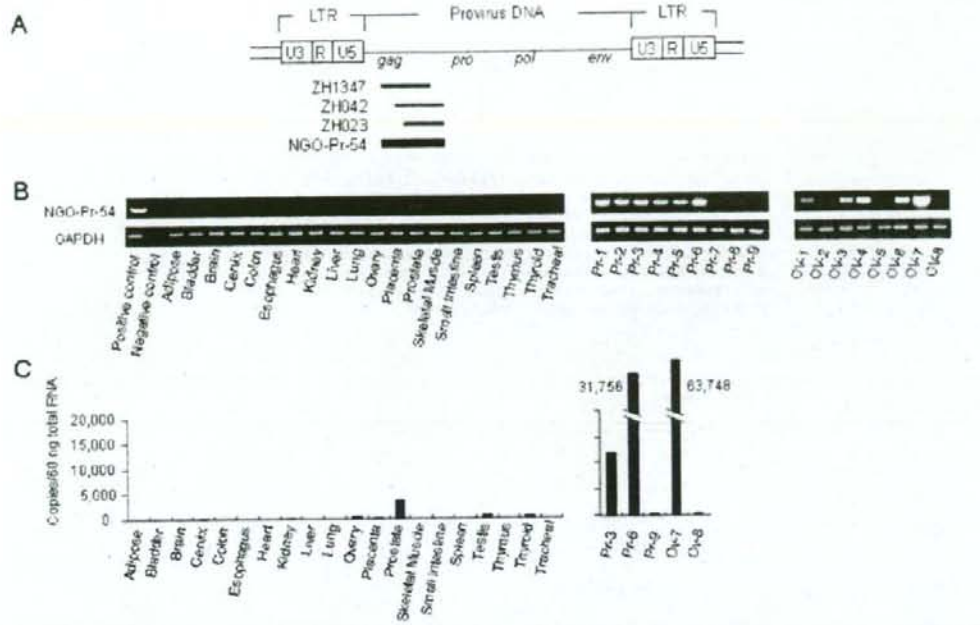

***NGO-Pr-54* mRNA expression in normal and tumor tissues.** (A) Genomic structure of the HERV-K provirus. The HERV-K provirus contains the *gag*, *pro*, *pol*, and *env* genes flanked by two long terminal repeats (LTRs). Three clones (ZH1347, ZH042, and ZH023) representing the same gene were recognized in prostate cancer cDNA libraries by SEREX using autologous sera; the gene was named *NGO-Pr-54*. (B) RT-PCR results for *NGO-Pr-54* mRNA in a panel of normal tissues (left), prostate cancer (middle, Pr-1 to -9), and ovarian (right, OV-1 to -8) cancer specimens. (C) Quantitative real-time RT-PCR for a panel of normal tissues (left) and prostate and ovarian cancer specimens (right).

Results

Identification of the *NGO-Pr-54* gene in prostate cancer by SEREX using autologous serum

The prostate cancer specimens were obtained surgically from an 80 year-old patient and cDNA expression libraries were constructed from the mRNA. A total of 1.3×10^6 cDNA clones were prepared. Approximately 2.0×10^5 clones were screened with the autologous patient serum using SEREX methodology and 125 reactive clones were isolated. These clones correspond to 67 different genes, as determined by nucleotide sequencing analysis. As shown in Figure 1A, three clones (ZH1347, ZH042, and ZH023) represented the same gene which was named *NGO-Pr-54* and which was found to be a part of the human endogenous retrovirus-K (HERV-K) element on chromosome 22q11.2 (GenBank accession number AP000346). The expression sequence tag (EST) database indicated a restricted expression pattern for *NGO-Pr-54* in normal prostate tissue.

NGO-Pr-54 mRNA expression in normal and tumor tissues and in tumor cell lines

NGO-Pr-54 mRNA expression was investigated in a panel of normal tissues, tumors, and tumor cell lines by 35 cycle RT-PCR using specific primers. As *NGO-Pr-54* contains no intron, the RNA was pretreated with DNase to remove genomic DNA before reverse transcription. As shown in Figure 1B, *NGO-Pr-54* mRNA was faintly detectable in normal prostate. Quantitative real-time RT-PCR analysis confirmed the results (Figure 1C). In tumors, *NGO-Pr-54* mRNA was observed to be strongly expressed in 6/9 prostate cancers, 5/8 ovarian cancers, and 5/14 leukemias (Figure 1B). Table 1 summarizes *NGO-Pr-54* mRNA expression in various tumors and tumor cell lines as determined by RT-PCR analysis.

Production of monoclonal antibody (mAb) against NGO-Pr-54

By phage plaque assay, 16/31 sera samples from prostate cancer patients reacted with NGO-Pr-54, but none of 30 control sera from healthy donors did. Within the three clones, ZH042 constantly gave a strong reaction despite lacking the N-terminal sequence of the putative ORF (715 amino acids) of *NGO-Pr-54* (Figure 2A). Therefore, a recombinant protein consisting of the C-terminal 438 amino acids was produced and BALB/c mice were immunized with the protein to produce a mAb. Five clones were obtained: Three IgG1 and two IgG2. TI-35 mAb, which was IgG1, reacted strongly to the recombinant protein. Figure 2B shows the titration curve of the TI-35 mAb obtained by ELISA using the recombinant protein.

Figure 2

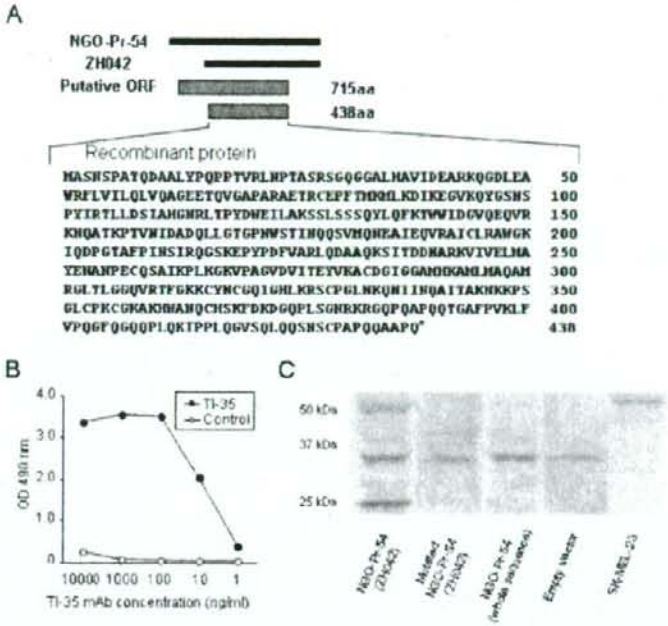

Production of a monoclonal antibody, TI-35, against NGO-Pr-54. (A) Schematic representation of *NGO-Pr-54* and its putative open reading frame (ORF). The recombinant protein was produced from the C-terminal 438 amino acids of the putative ORF. (B) Reactivity of monoclonal antibody TI-35 against recombinant NGO-Pr-54 protein. Control, isotype (IgG1) matched mouse mAb (anti-Lyt-2.1). (C) Western blot of the lysate of 293T cells transfected with NGO-Pr-54 (ZH042) plasmid, mutated NGO-Pr-54 (ZH042) plasmid with a point mutation in the start codon (ATG to TTG), NGO-Pr-54 (whole sequence) plasmid, and empty vector (only p3xFLAG-CMV-14), and SK-MEL-23 using TI-35 mAb.

Table 1

***NGO-Pr-54* mRNA expression in tumors and tumor cell lines.**

Tumor Specimens and Cell Lines	Positive / Total
Esophageal cancer	0/73
Gastric cancer	2/83
Hepatocellular carcinoma	1/42
Leukemia	5/14
Lung cancer	0/21
Lymphoma	0/3
Ovarian cancer	5/8
Prostate cancer	0/9
Rhabdomyosarcoma	2/2
Colon cancer cell line	4/8
Leukemia cell line	1/1
Lung cancer cell line	0/10
Melanoma cell line	3/7
Mesothelioma cell line	1/4
Prostate cancer cell line	0/3

NGO-Pr-54 protein expression in 293T transfectants and SK-MEL-23 by Western blot analysis

We examined NGO-Pr-54 protein expression in the transfectants by Western blot using TI-35 mAb. As shown in Figure 2C, TI-35 mAb recognized two bands of approximately 50 kDa and 20 kDa in the 293T lysate when transfected with the NGO-Pr-54 (ZH042) plasmid. The 50-kDa band size corresponds to the fusion protein of NGO-Pr-54 and FLAG-tag. Insertion of a point mutation in the start codon from ATG to TTG in NGO-Pr-54 (ZH042) (mutated NGO-Pr-54 (ZH042) plasmid) resulted in no bands being detectable in the 293T lysate. The 50-kDa band was also detected in the lysate of a melanoma cell line, SK-MEL-23, in which *NGO-Pr-54* mRNA expression had been detected by RT-PCR.

On the other hand, TI-35 mAb detected no NGO-Pr-54 protein in the 293T lysate when transfected with *NGO-Pr-54* (whole sequence) including the putative ORF.

Subcellular localization of NGO-Pr-54

The subcellular localization of NGO-Pr-54 was investigated using 293T and COS7 cells transfected with *NGO-Pr-54* (ZH042) by indirect immunofluorescence. As shown in Figure 3A, staining was observed in non-permeabilized 293T and COS7 transfectants by either TI-35 mAb or anti-FLAG mAb. Control staining of the membrane by rhodamine-labeled

Figure 3

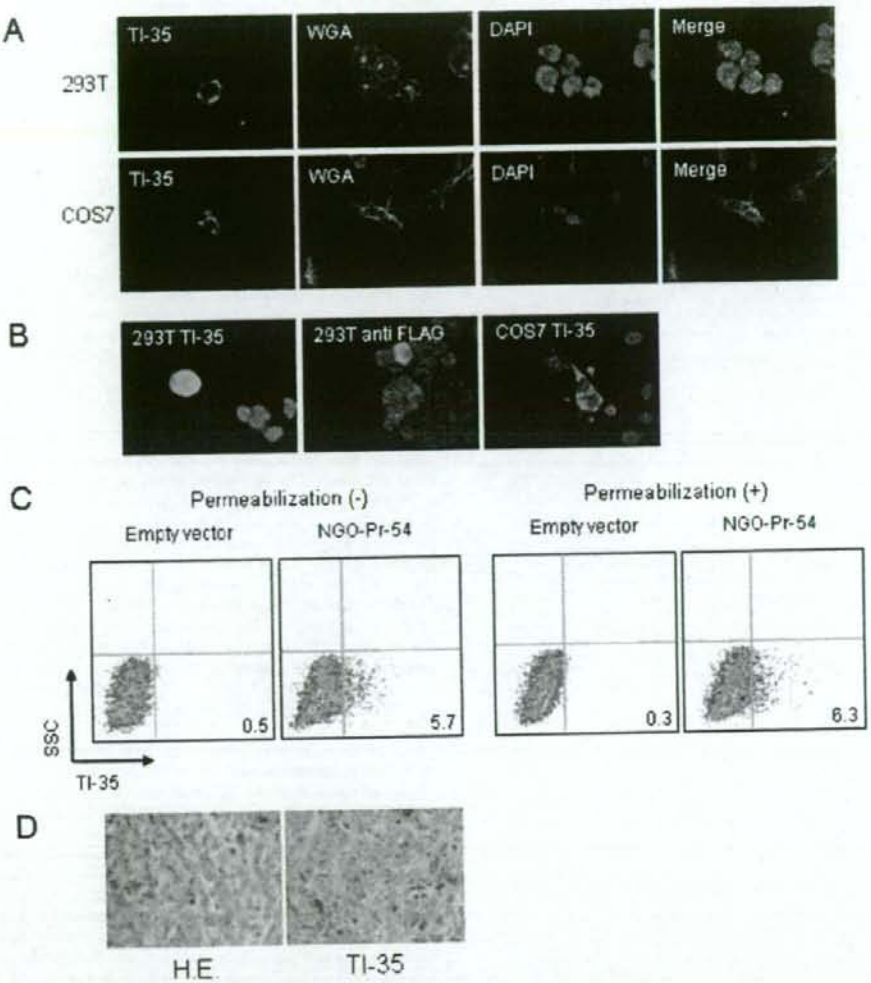

Subcellular localization of NGO-Pr-54 protein. (A) Immunofluorescence staining of 293T and COS7 transfected with NGO-Pr-54 (ZH042) plasmid without permeabilization. TI-35 and anti-FLAG antibody (not shown) detected NGO-Pr-54 protein (green) similarly. The cell membrane was marked with rhodamine-labeled WGA (red) and the nuclei were stained with DAPI. (B) 293T and COS7 cells were stained with TI-35 mAb and anti-FLAG antibody after permeabilization. (C) Flow cytometry analysis of 293T cells transfected with *NGO-Pr-54* (ZH042) using TI-35 mAb with or without permeabilization: (D) Hematoxylin and eosin (H&E) and TI-35 mAb staining of a melanoma specimen obtained from a patient showing an antibody against NGO-Pr-54. Magnification, 400x.

WGA gave similar results. In permeabilized cells, cytoplasmic staining was also observed (Figure 3B). As shown in Figure 3C, flow cytometry analysis confirmed the cell surface expression of NGO-Pr-54 protein.

A melanoma specimen obtained from a patient who showed antibody against the recombinant NGO-Pr-54 was examined further by immunohistochemistry. As shown in Figure 3D, diffuse staining possibly involving the cytoplasm and membrane was observed in the tumor cells.

Antibody response against NGO-Pr-54 in cancer patients

The antibody response against NGO-Pr-54 was investigated in cancer patients by ELISA using recombinant protein. Figure 4 shows the titration curves for positive sera from two prostate cancer patients, a melanoma patient, and serum from a healthy donor. The results are summarized in Table 2. Antibody against NGO-Pr-54 was found in sera from bladder, liver, lung, ovarian,